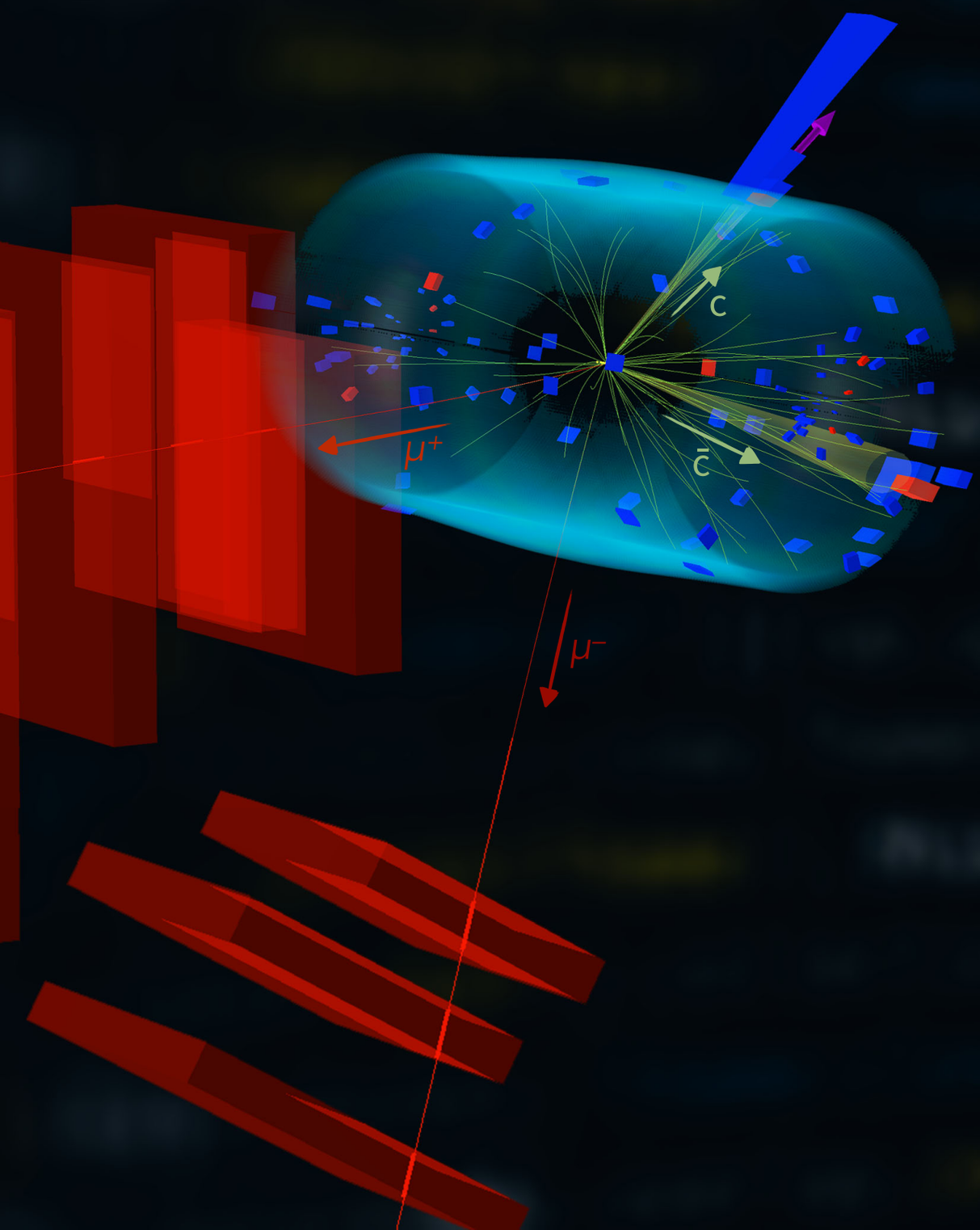

Constraining the Higgs-charm coupling at CMS

Based on arXiv:2205.05550, CMS-PAS-HIG-21-008

Congqiao Li (李聪乔), *Peking University*
on behalf of the CMS Collaboration

Higgs Potential 2022 · Peking University, Beijing
25 July, 2022

Motivation

- ➔ Measurement of the Higgs boson properties is of vital importance since its discovery
  - ❖ couplings with 3rd generation fermions (t/b/τ) well-measured in high precision
- ➔ Next milestone: measure Yukawa couplings with 2nd generation fermions
  - ❖ **Higgs-charm** coupling can be modified in some BSM scenarios → essential to verify SM prediction and find possible hints to BSM
  - ❖ direct approach: **measure Higgs-charm coupling via H→cc decay channel**

Higgs coupling measurement

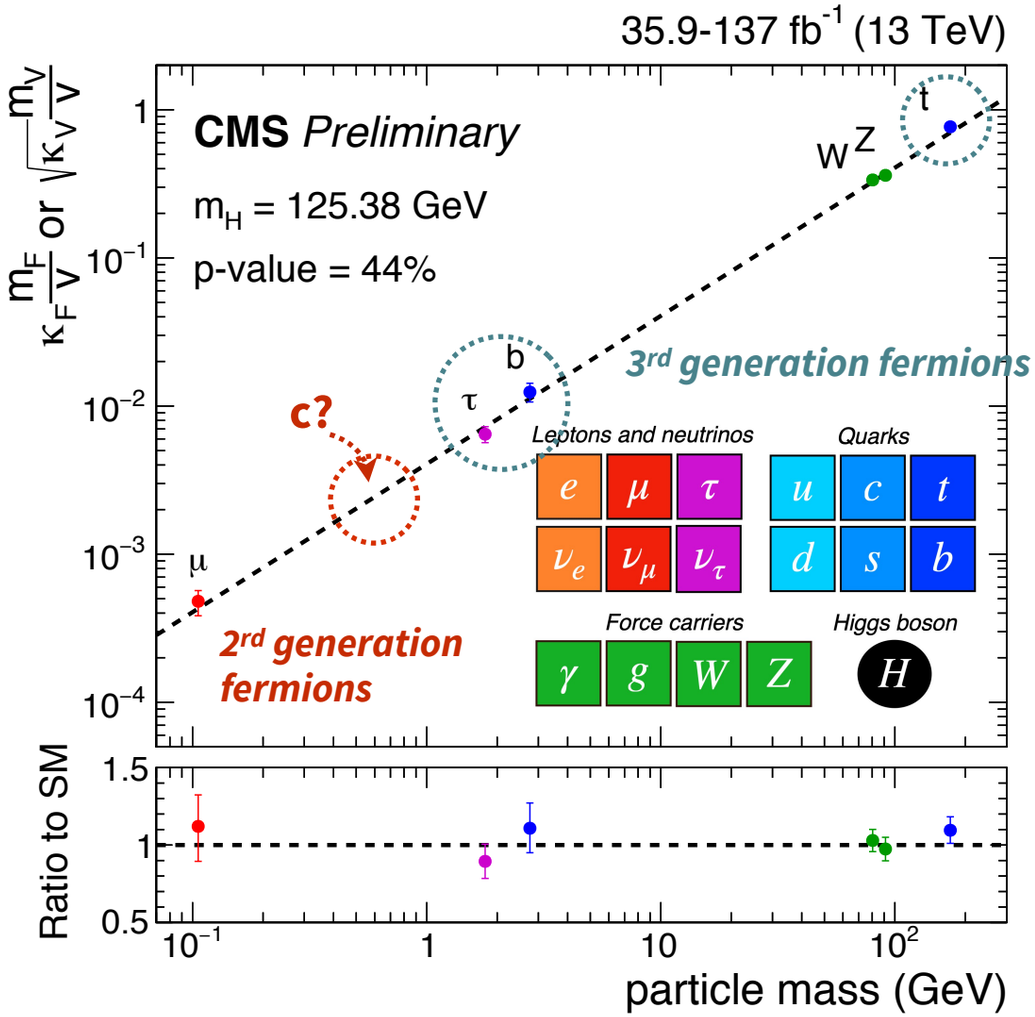

Journey of VHcc search

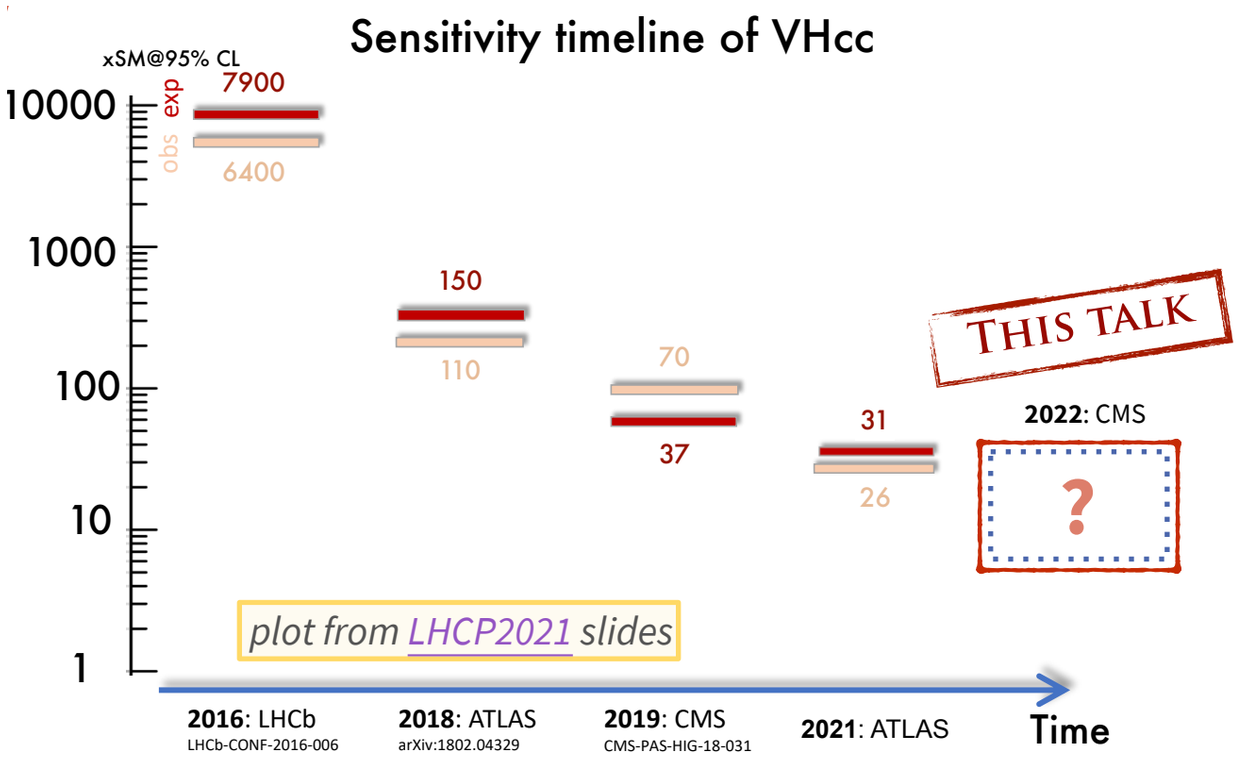

➔ **VH(→cc) mode** with V= W(→ℓν) or Z(→ℓℓ/νν) is most sensitive channel by far

- ❖ leptonic decay of W/Z provides a handle to suppress multijet background

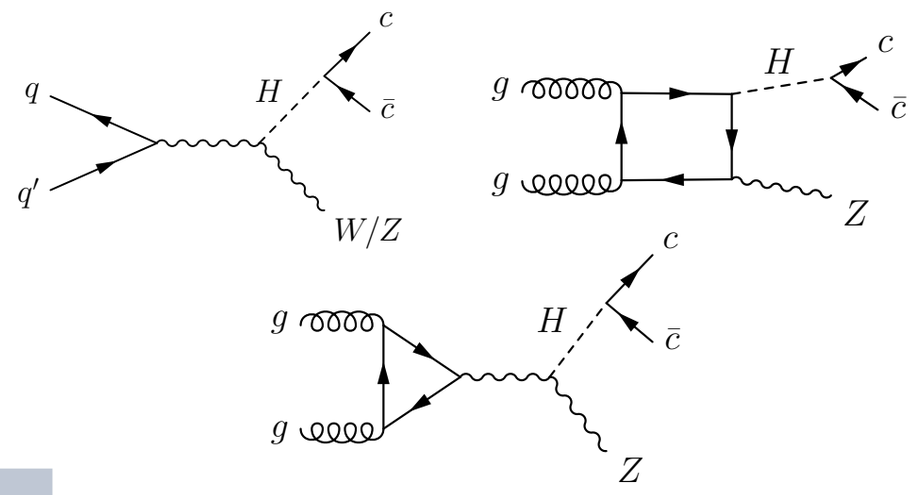

OBS (EXP) UL σ(VHcc)	OBS (EXP) UL on κ_c	∫*Ldt*	
μ < 110 (150)	-	36.1 fb^{-1} (2016)	ATLAS [*PRL 120 (2018) 211802*] Z(→ℓℓ)H
μ < 70 (37)	-	35.9 fb^{-1} (2016)	CMS [*JHEP 03 (2020) 131*] V(Z→ℓℓ, Z→νν, W→ℓν)H
μ < 26 (31)	$\lvert\kappa_c\rvert$ < 8.5 (12.4)	139 fb^{-1} (full Run 2)	ATLAS [HIGG-2021-12] V(Z→ℓℓ, Z→νν, W→ℓν)H
?	?	138 fb^{-1} (full Run 2) THIS TALK	CMS [arXiv:2205.05550 (accepted by PRL)] [CMS-PAS-HIG-21-008] V(Z→ℓℓ, Z→νν, W→ℓν)H

CMS VHcc search using 2016 data

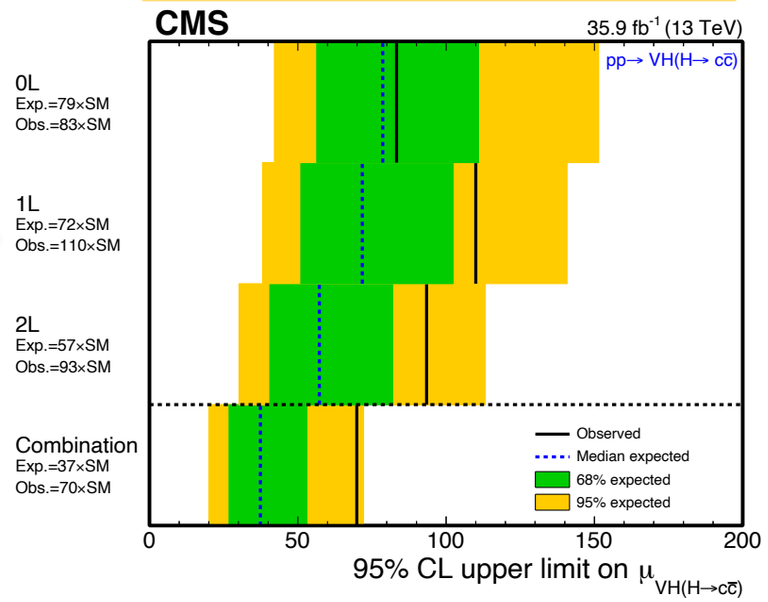

VHcc analysis in a nutshell

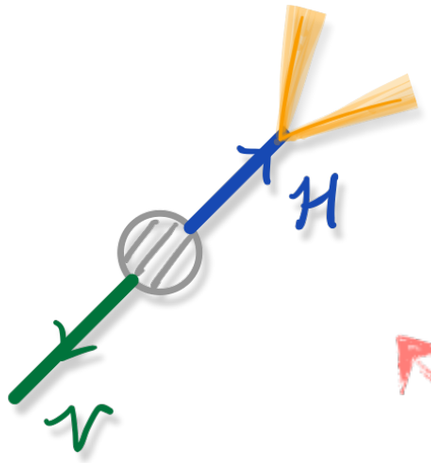

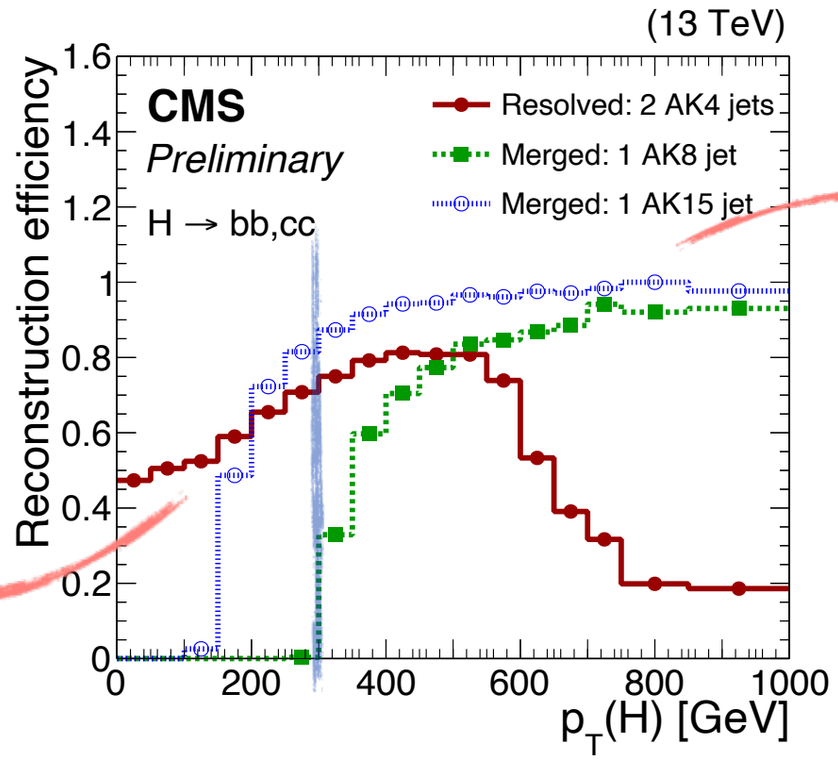

NEW PHASE-SPACE EXPLORE IN CMS

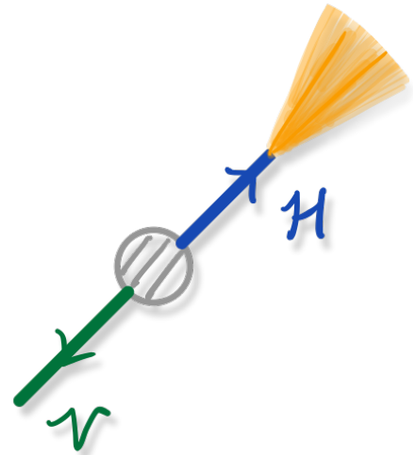

$\Delta R(c, c) \sim 2m(H)/p_T(H)$

Resolved-jet topology

- reconstruct H→cc decay with two *R*=0.4 jets
- apply charm tagger (DeepJet) for each jet
- able to probe larger fractions of the available phase space (~95%)

Merged-jet topology

- reconstruct H→cc decay with one large-*R* (*R*=1.5) jets
- apply a di-charm tagger (ParticleNet X→cc) to the jet; able to exploit the correlations of two charms
- improved signal purity with large $p_T(H)$

Merged-jet: H→cc identification with ParticleNet

➔ Merged jet topology: Higgs candidate reconstructed by a single large-*R* jet

❖ major improvement has been made in improving on the tagger tagger to identify H→cc in one large-*R* jet

JHEP 03 (2020) 131 (2016 analysis)

DeepAK8 (DeepAK15) [JINST 15 (2020) P06005]

- ❖ multi-class DNN classifier with 1D convolutional neural network
- ❖ directly uses jet constituents (particle-flow candidates / secondary vertices)
- ❖ mass decorrelation via adversarial training

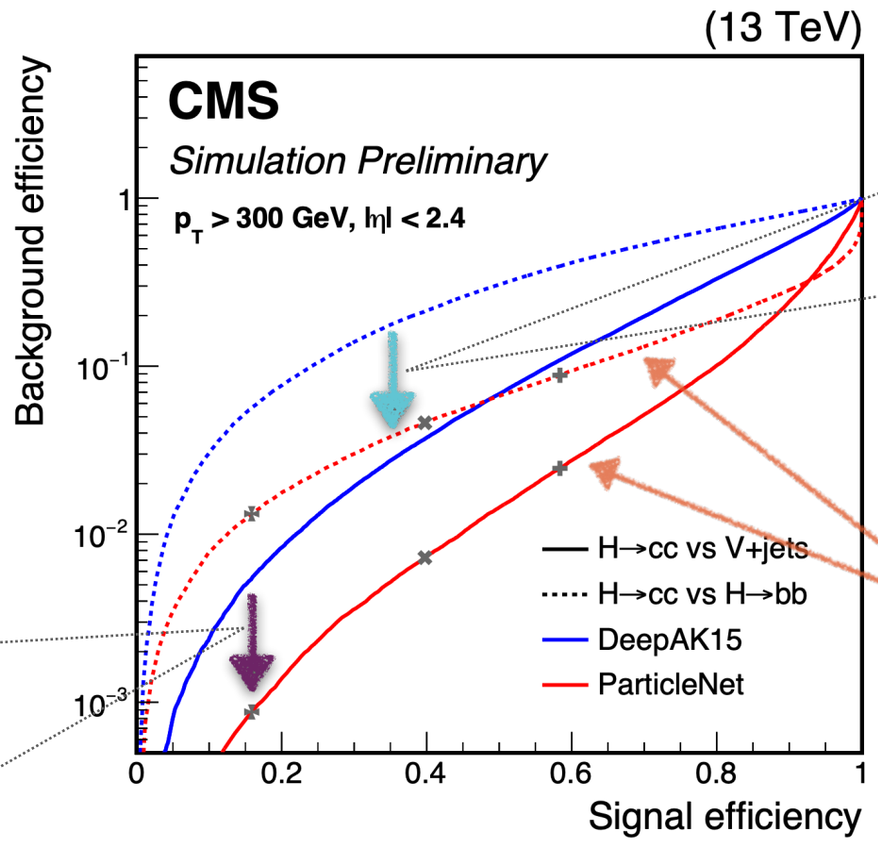

~5x better H→bb rejection

~5x better V+jet rejection

CMS-PAS-HIG-21-008 (Run 2 analysis)

ParticleNet [CMS-DP-2020-002]

- ❖ same spirit as DeepAK8, but substantially improved:
- ❖ **graph neural network architecture**
- ❖ **novel mass decorrelation technique**

→ details in the next slide

Merged-jet: ParticleNet

➔ ***ParticleNet***: an advanced multi-class jet classifier with a graph neural networks (**GNN**) structure, processing input features on a "**point cloud**" [CMS-DP-2020-002]

- ❖ **point cloud:** an unordered set of particles
- ❖ **GNN**: apply the EdgeConv operation on the point cloud
- ❖ able to use **low-level jet features** as inputs (particle-flow candidates & secondary vertices)

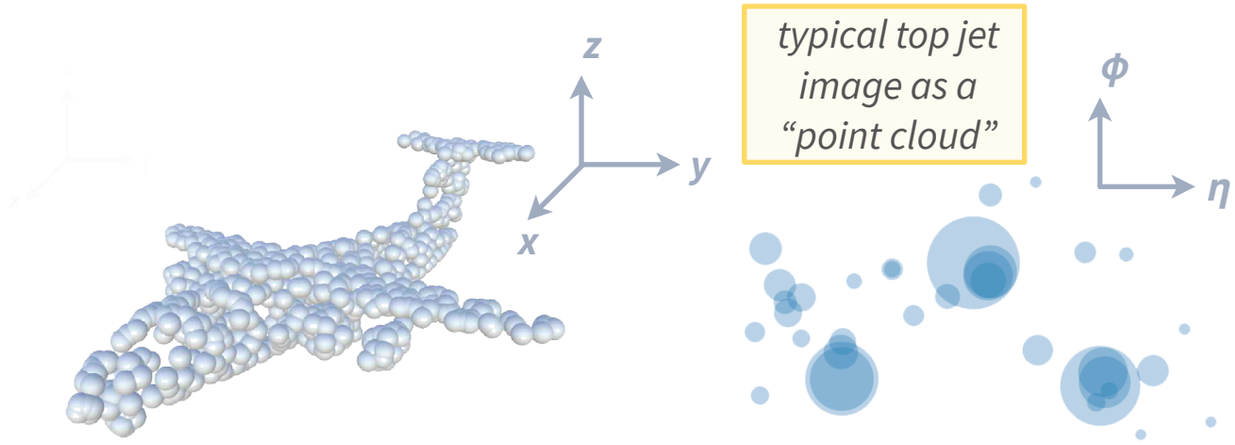

➔ Details and techniques:

- ❖ **categorisation**: resonance decaying to different flavour contents & QCD:
  - X→bb, X→cc, X→qq, QCD (bb, cc, b, c, others)
- ❖ **mass decorrelation** (decorrelate with Higgs mass): signal & QCD reweighted on a flat (p_T, mass) distribution before training
- ❖ **novel calibration method**: select a phase-space from g→cc that resembles H→cc jets, by vetoing jets with large gluon contamination using a BDT [CMS-DP-2022-005]

ParticleNet mass-decorrelation effect

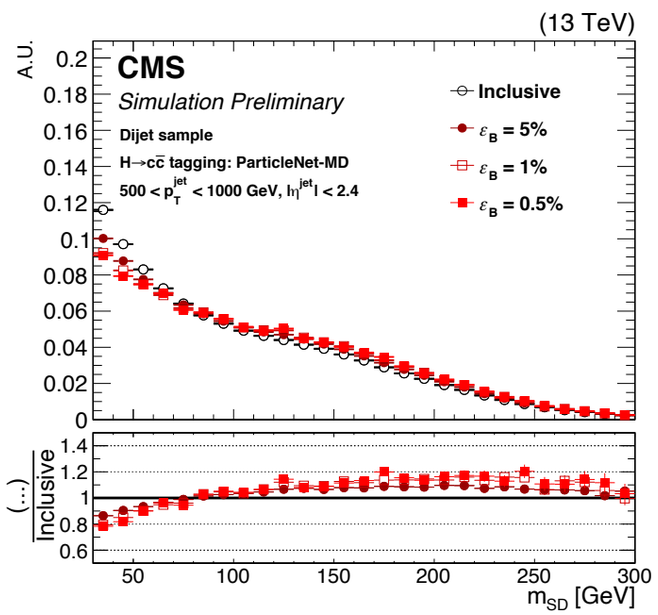

tagger calibration: use BDT to select a phase-space from g→cc

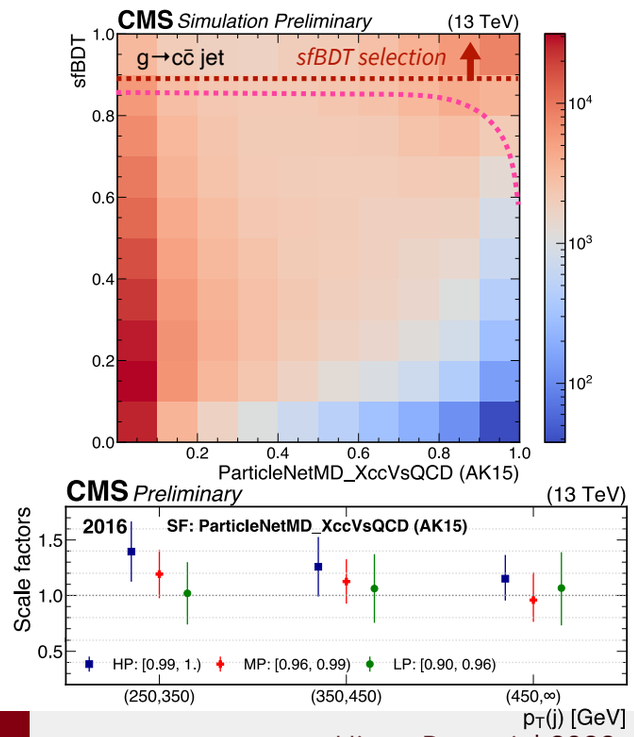

Merged-jet: analysis techniques

➔ ParticleNet for cc-tagging on large-R (R=1.5) jets

- ✓ **huge improvement**: ~5 times increase in BKG rejection w.r.t. DeepAK15 tagger (2016) [CMS-DP-2020-002]
- ✓ tagger calibration with novel BDT approach [CMS-DP-2022-005]

➔ Di-charm jet mass regression

- ❖ use the ParticleNet architecture with a regression layer [CMS-DP-2021-017]
- ❖ ~20–25% improvement in exp. upper limit, w.r.t. using soft-drop mass

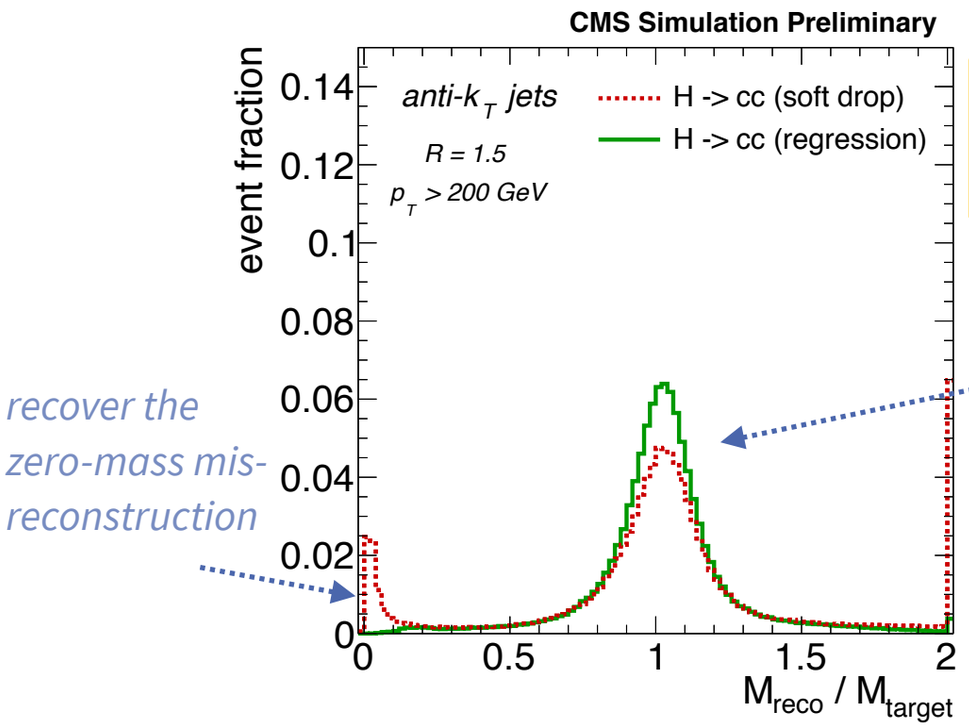

soft-drop mass vs. regressed mass resolution

improved sensitivity with mass regression technique

recover the zero-mass mis-reconstruction

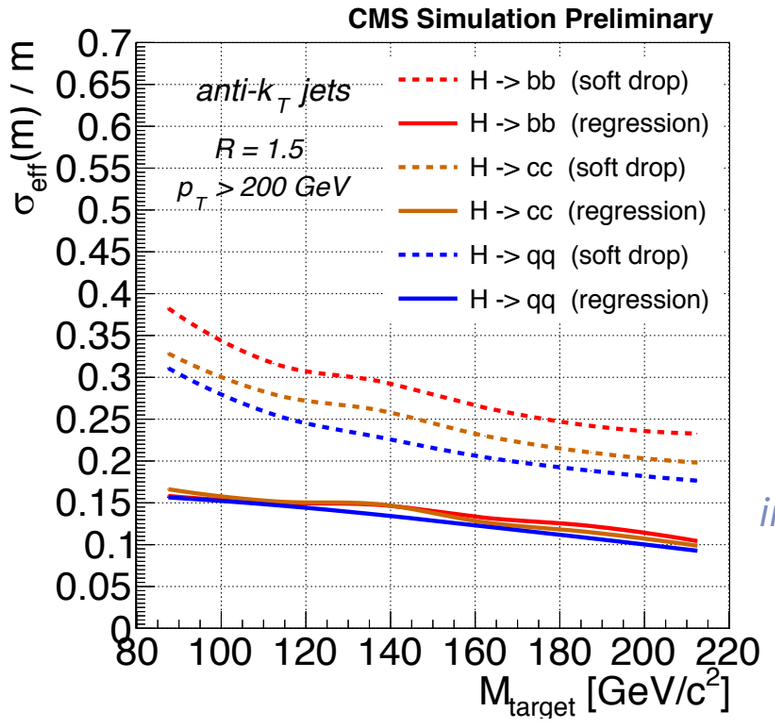

improved sensitivity

Merged-jet: analysis strategy

- ➔ train **kinematics BDTs** to separate VHcc signal vs. BKG
  - ❖ using only kinematics properties - no mass/flavour information
  - ❖ goal: **decorrelated BDT with H_{cand} mass and ParticleNet cc-tagging discriminant**
- ➔ CR defined by inverting the BDT cut
  - ❖ also define high N_j region for $t\bar{t}$
- ➔ apply **cc-tagging cut on three WPs**
- ➔ finally extract VHcc by **fitting on the regressed mass** variable

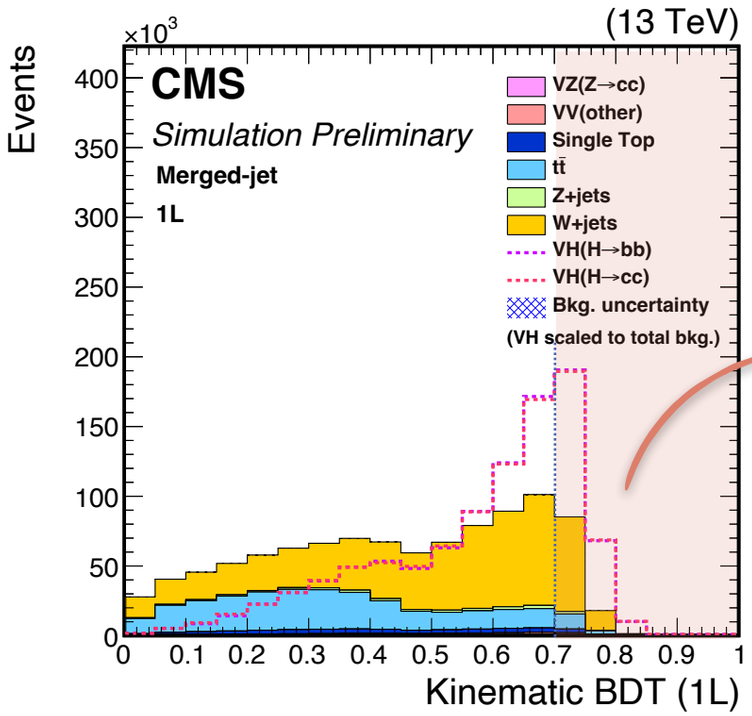

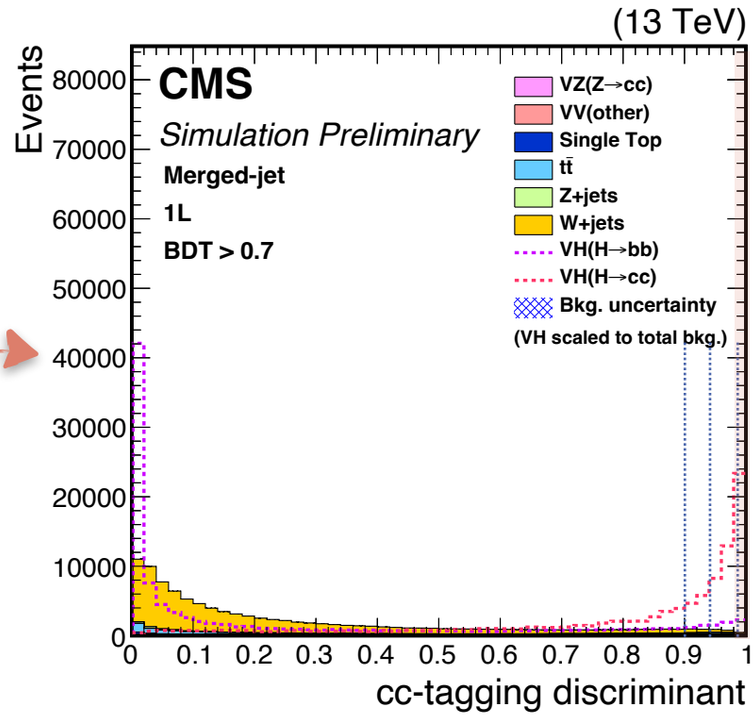

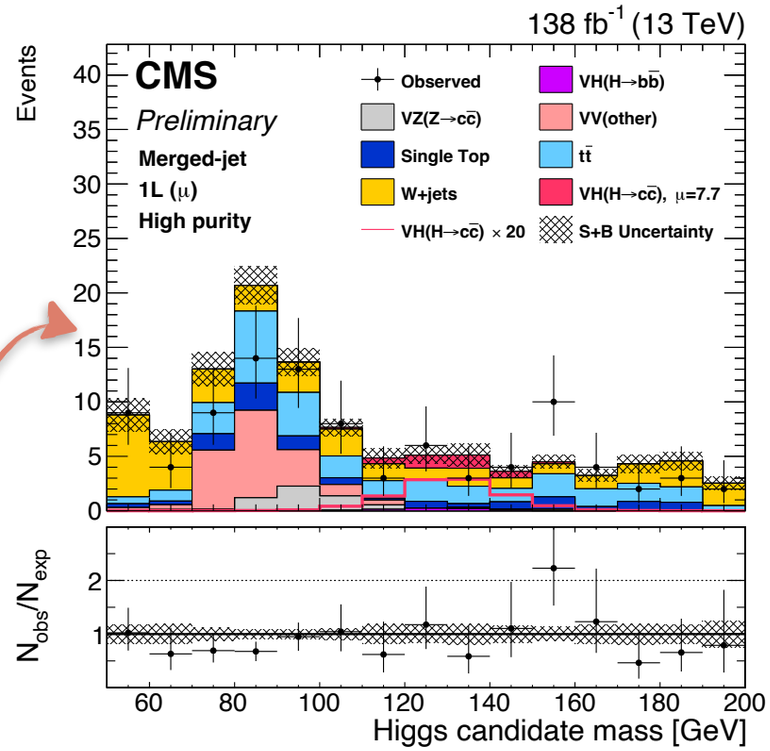

Merged-jet: CRs and SR

example post-fit plots for CR and SR, for 1L W(μν)

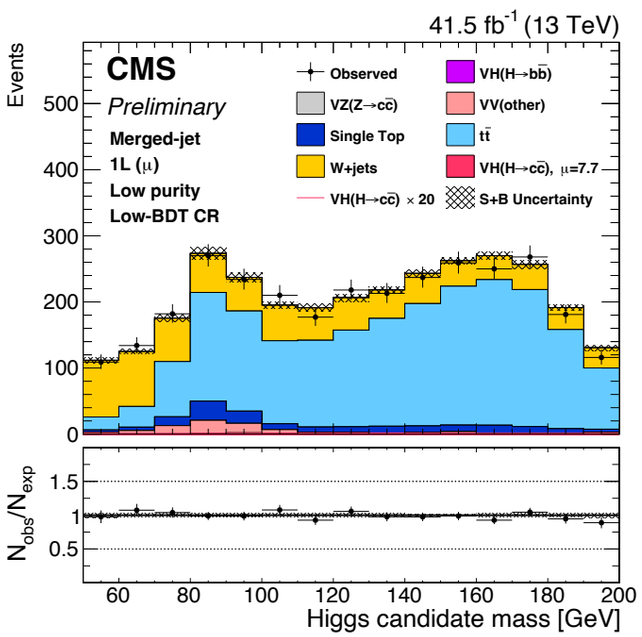

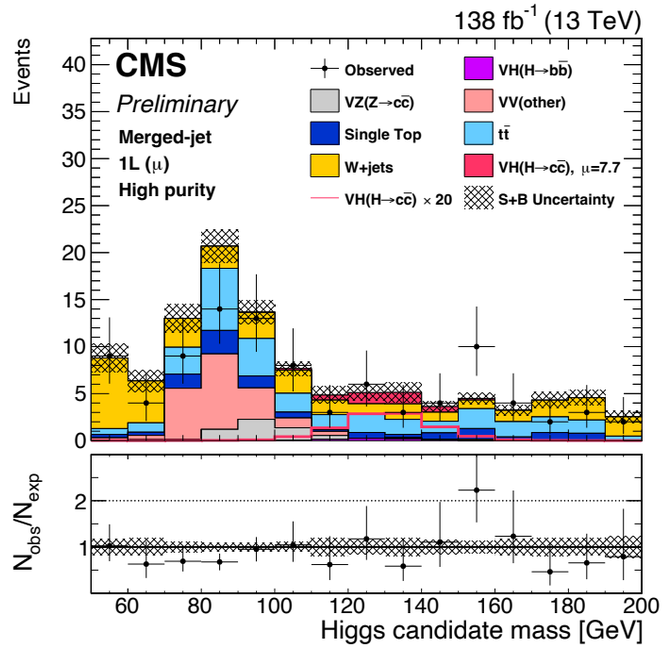

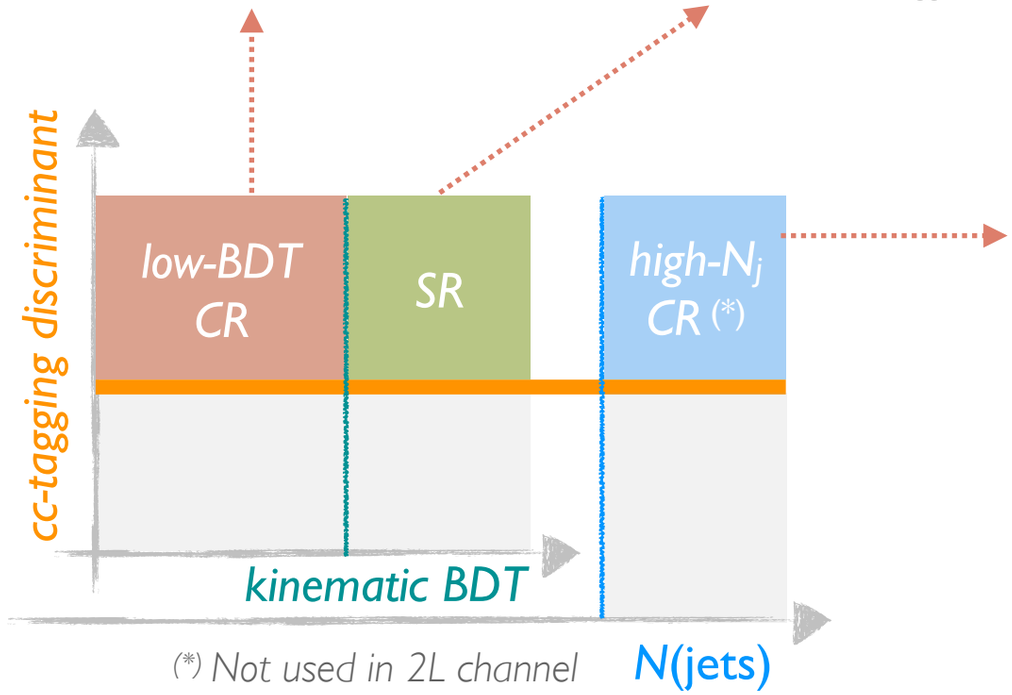

SR and CRs definition

- ➔ Plots shows High Purity WP of ParticleNet cc-tagger selection
  - ❖ the region that drives the sensitivity
- ➔ Simultaneous fit of all SR and CRs
  - ❖ extract BKG normalisation factors which are imposed to V+jets and tt̄ components

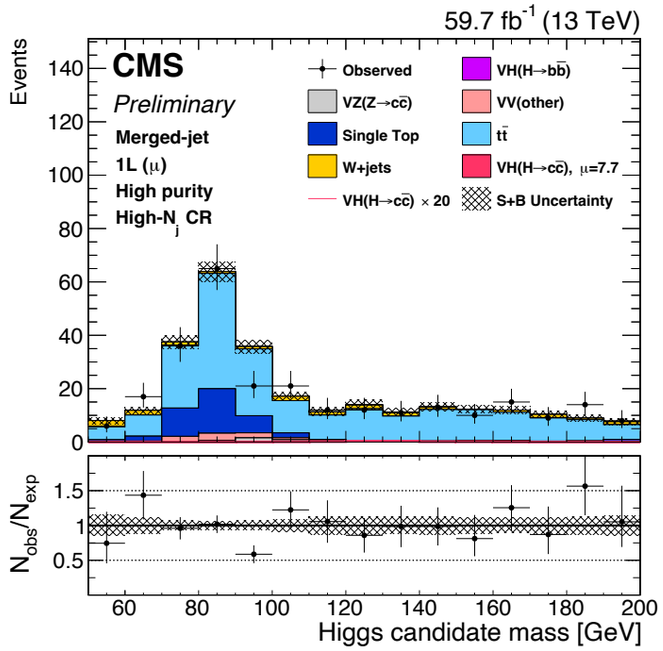

Resolved-jet: analysis techniques

➔ **Charm jet identification with DeepJet algorithm** [JINST 15 (2020) P12012]

- ❖ deep neural network in CNN+RNN structure
- ❖ two discriminants defined for c-jet vs. b-jet / light-jet separation
- ❖ ~2x (40%) improvements for light (b)jet rejection at 40% c jet efficiency w.r.t. DeepCSV (2016)

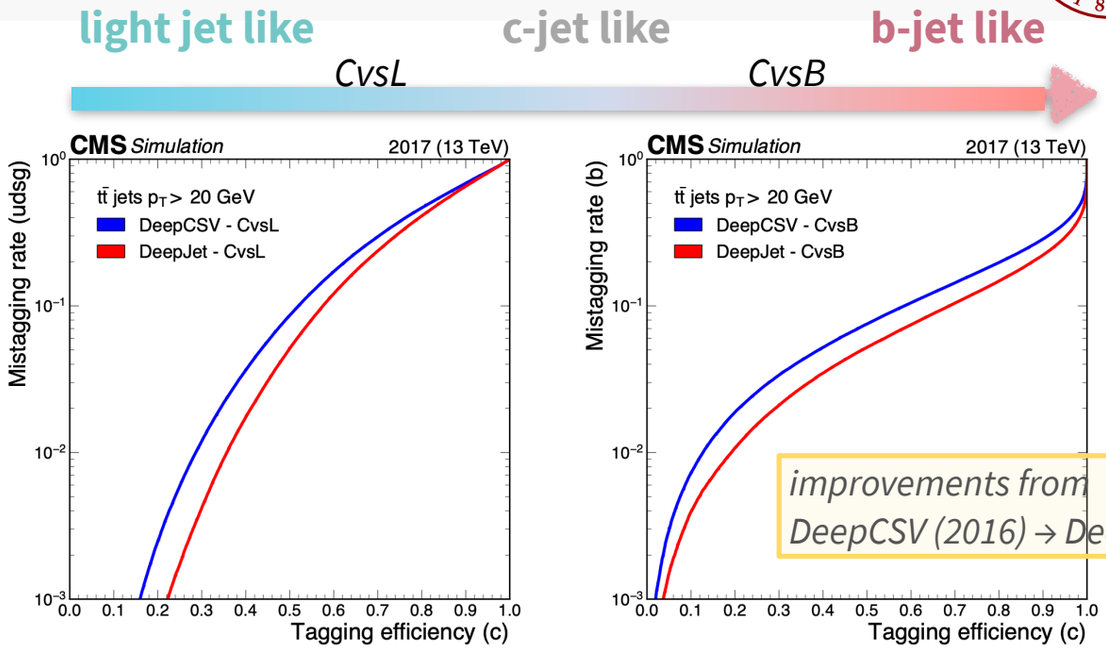

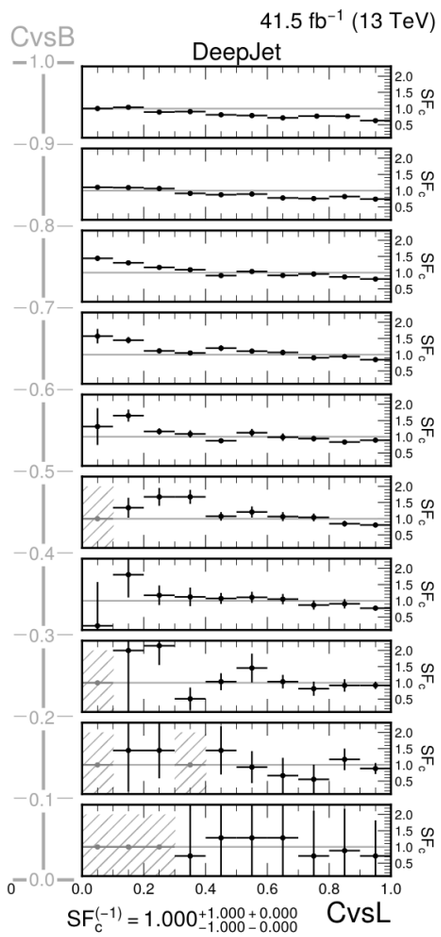

SF for entire c-tagging shape

improved mass resolution for on di-jet regressed mass

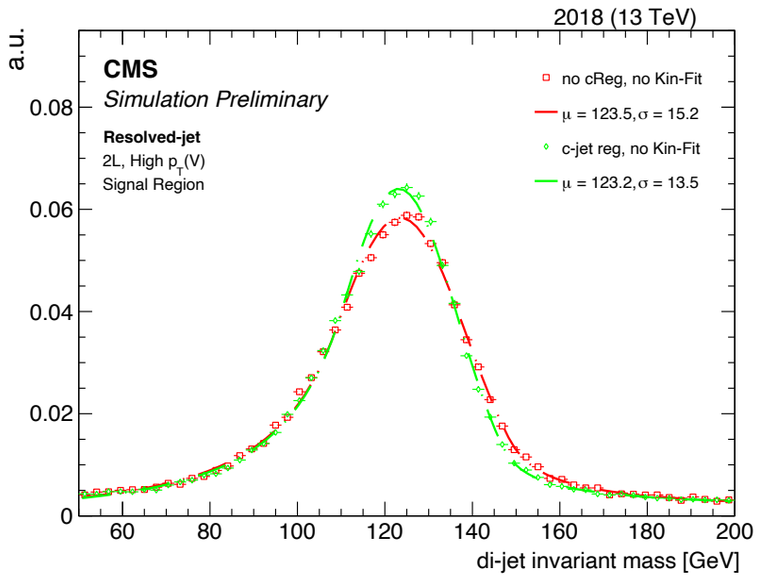

➔ **Novel charm tagger shape calibration** [JINST 17 (2022) P03014]

- ❖ correct the entire distribution of the c-tagging shape
- ❖ SF derived with an iterative approach using three samples enriched in light/b/c jet

➔ **Charm jet energy regression**

- ❖ regress RECO-to-GEN energy correction using DNN
- ❖ ~15% improvement in di-jet invariant mass resolution

Resolved-jet: analysis strategy

- ➔ define SR: two jets with **high c-tagging score**
- ➔ train **BDT** to separate VHcc signal vs. backgrounds
  - ❖ **kinematic fit** used in 2L: post-fit Z(ℓℓ)H(cc) system kinematics used as BDT input
- ➔ CRs defined for V+b/c/light jets, and $t\bar{t}$
  - ❖ by inverting c-tagger selection or vetoing Z/H_{cand} mass / requiring add. ℓ/jet
- ➔ finally extract VHcc signal by fitting on BDT
  - ❖ **simultaneous fit** on SR (on BDT) and all CRs (on c-tagging discriminant)

BDT to distinguish VHcc from backgrounds

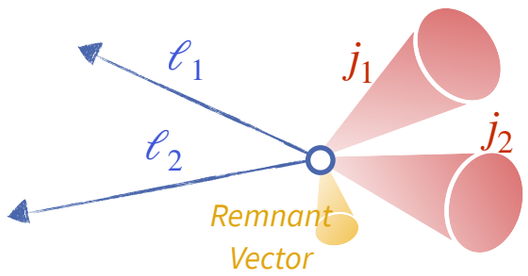

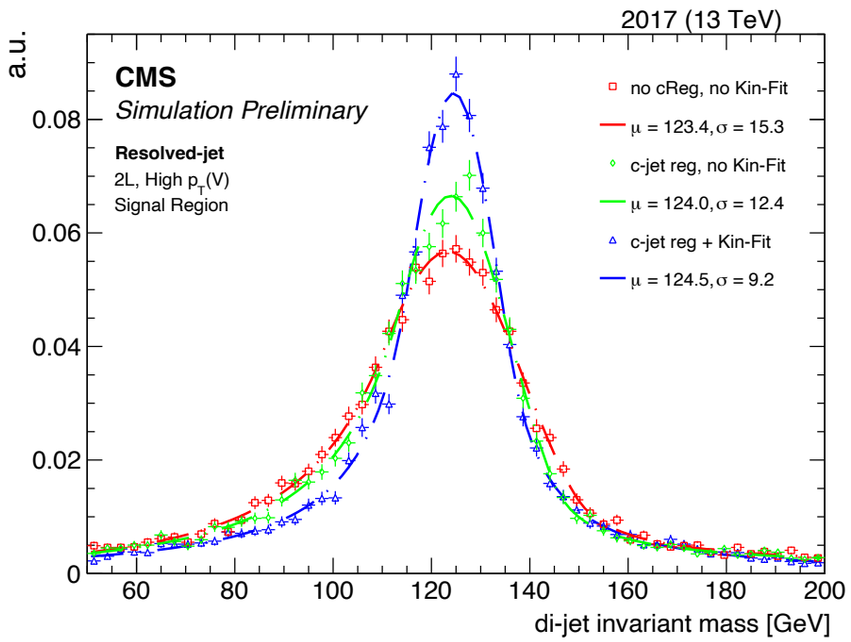

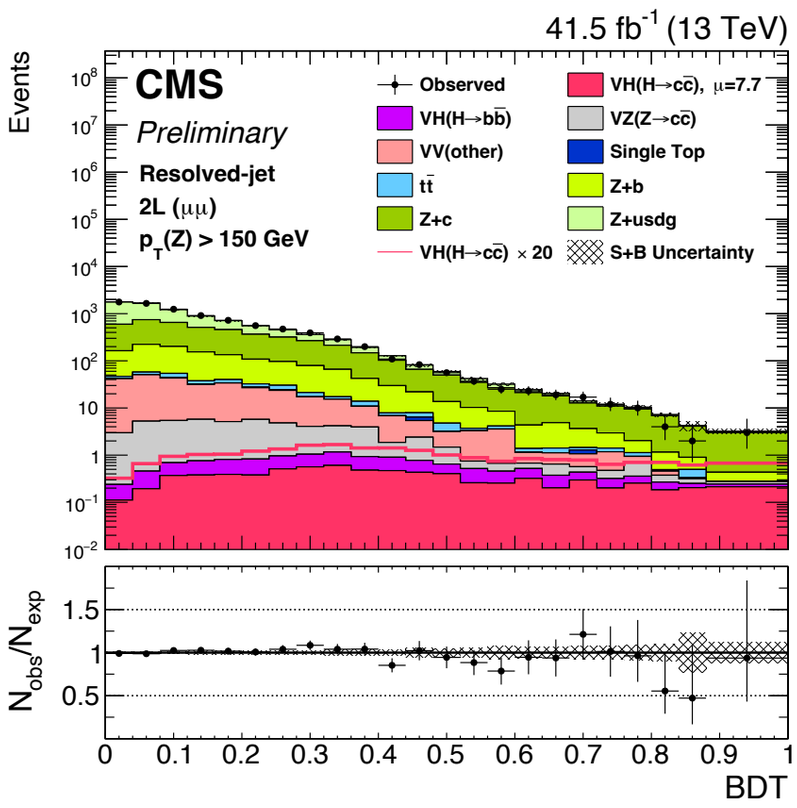

Resolved-jet: CRs and post-fit SR

example CR plots for 2L high-$p_T(V)$ channel, year 2017

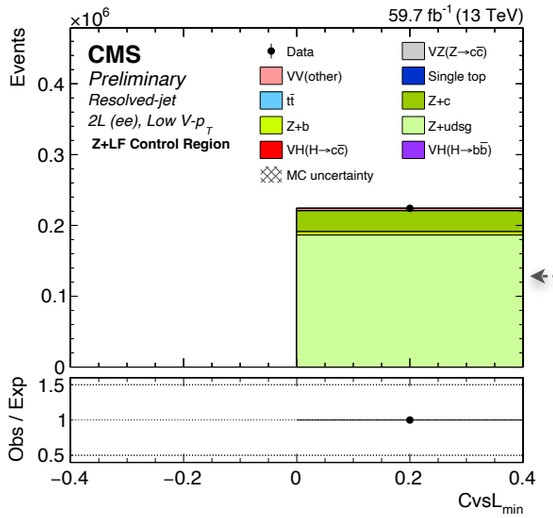

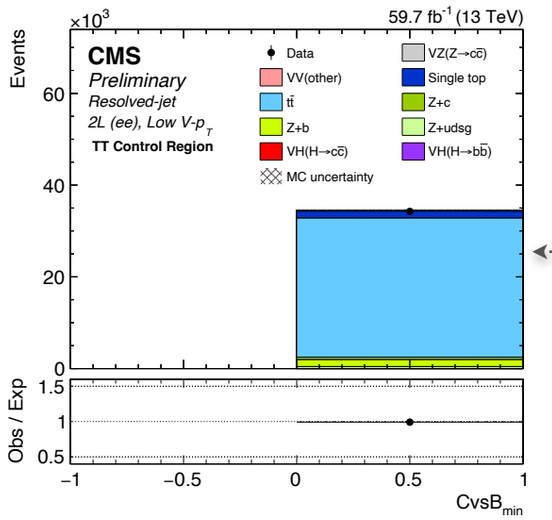

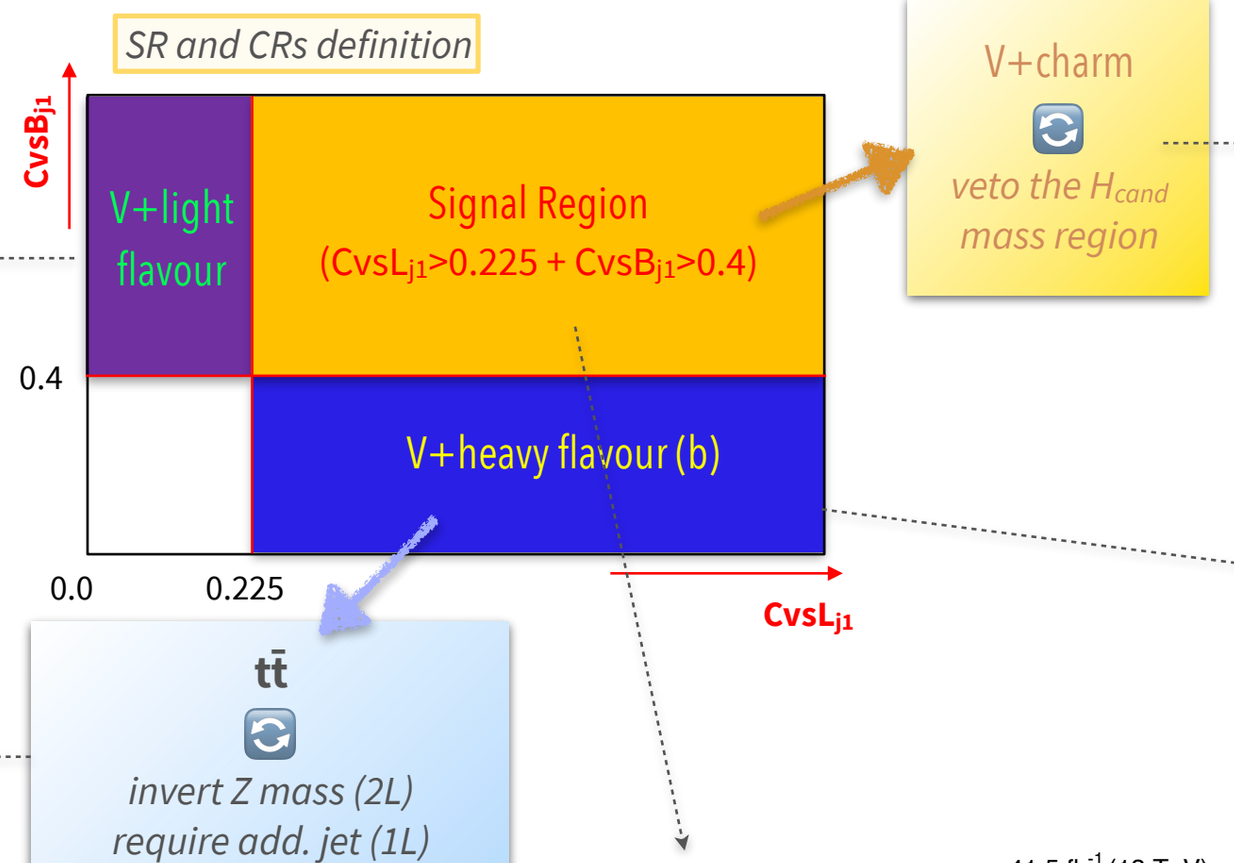

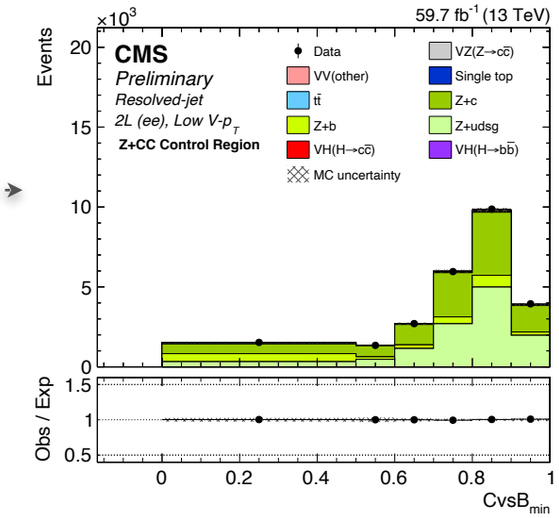

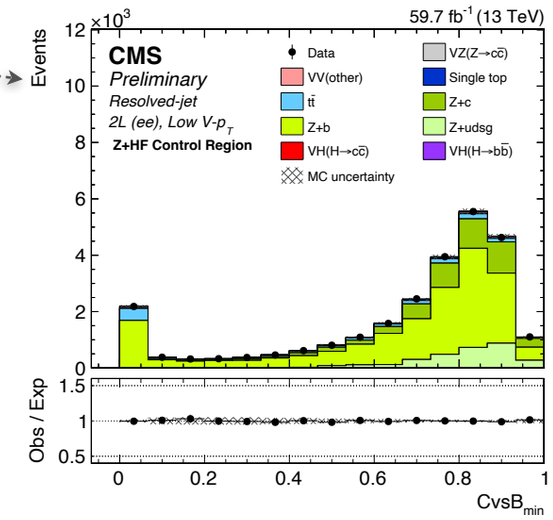

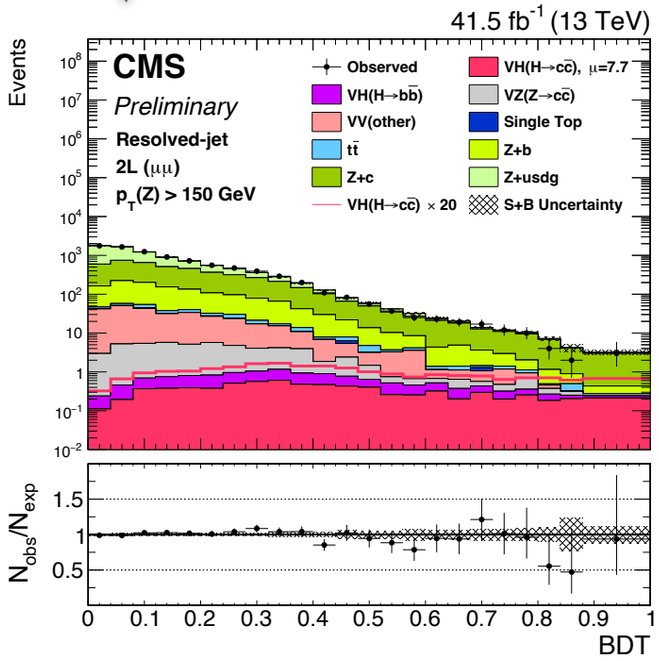

➔ Simultaneous fit in all SR and CRs

- **BKG normalisation factors** imposed to multiple components and extracted from the fit
- combined with merged-jet topology for the final signal extraction fit

SR plot (BKG impose norm factors extracted from CR-only fit)

Results from VZcc validation

RESULT

➔ Use VZcc analysis as a validation

- consider **VZcc process as the signal** and VHcc as the background
- apply with the same analysis and fit strategy (for resolved-jet analysis: re-train the BDT using VZcc as the signal)

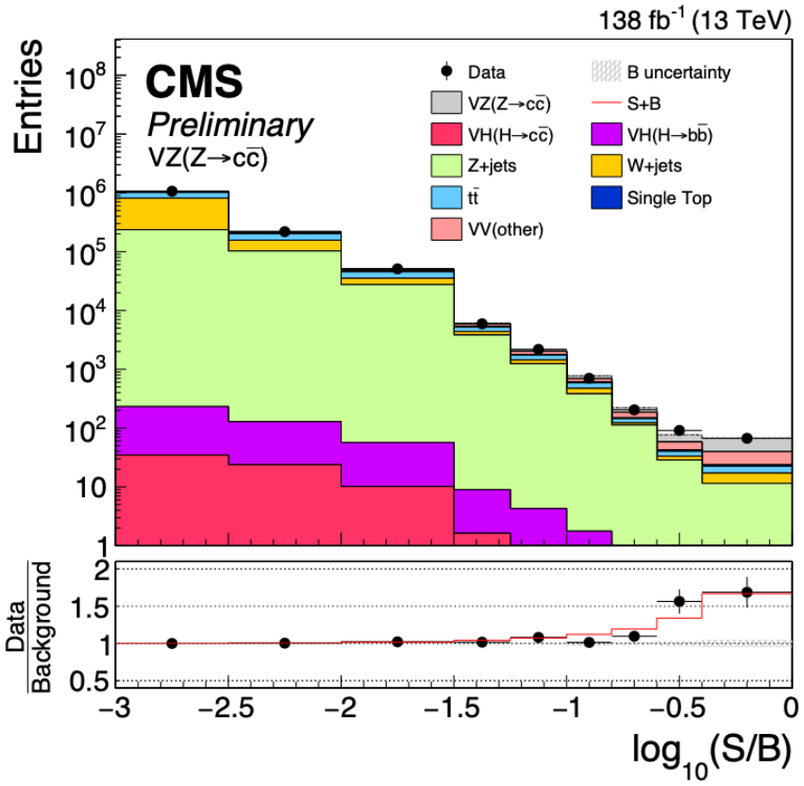

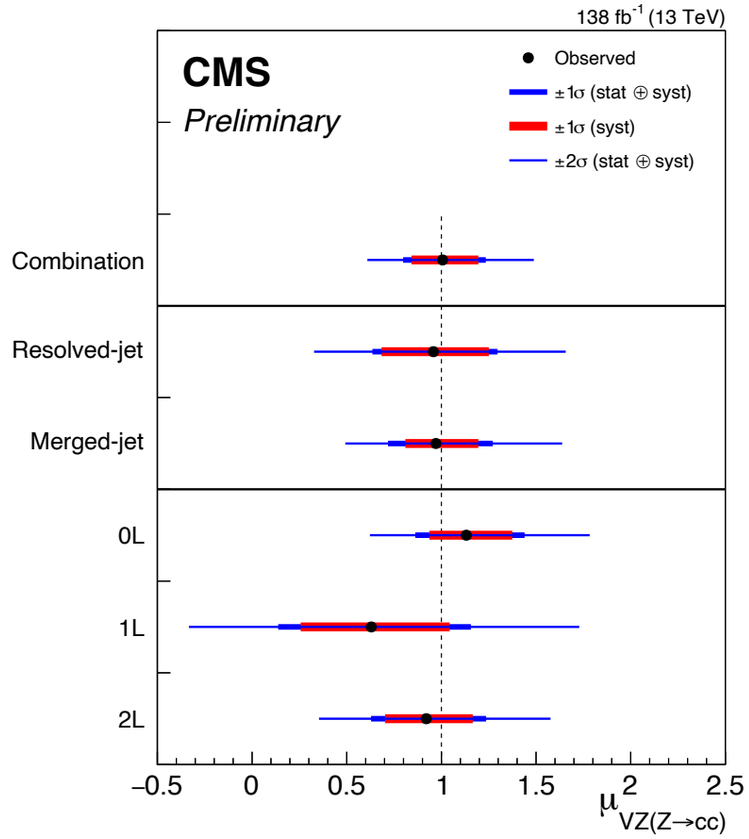

Observed significance for VZ(Z → cc): **5.7σ**

- expected significance: 5.9σ

First observation of Z→cc at a hadron collider!

Best-fit signal strength: $\mu_{VZ(Z \to cc)} = 1.01^{+0.23}_{-0.21}$

- very good agreement with SM expectation
- consistent results between topologies/channels

VHcc results

RESULT

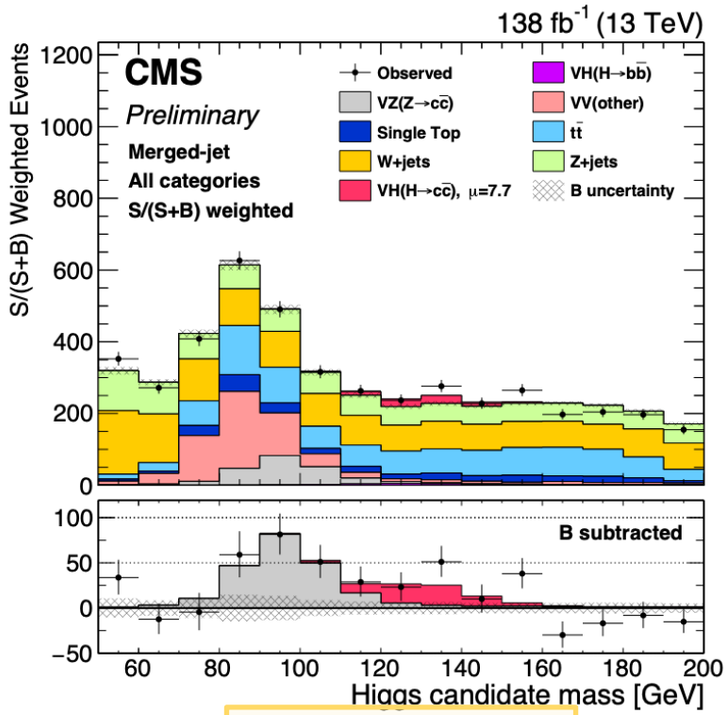

merged-jet topology

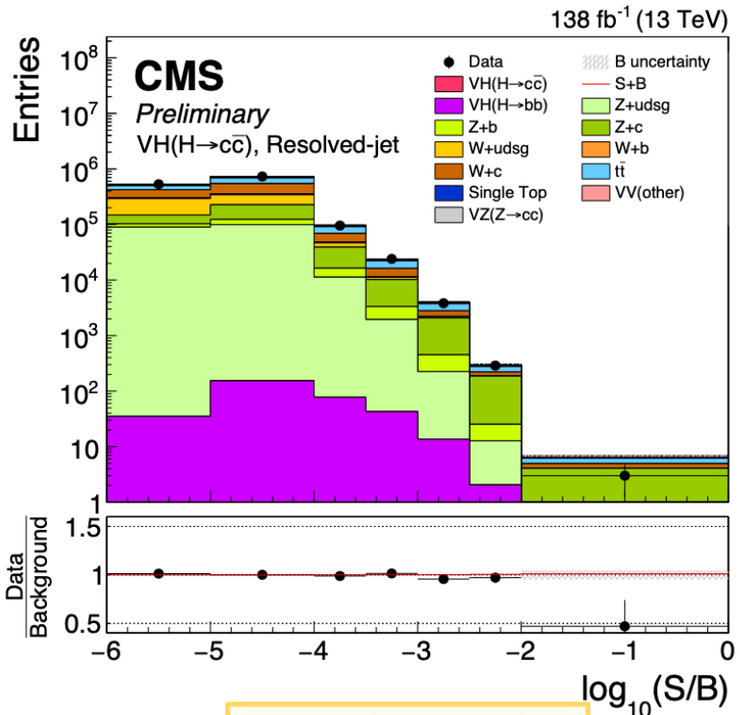

resolved-jet topology

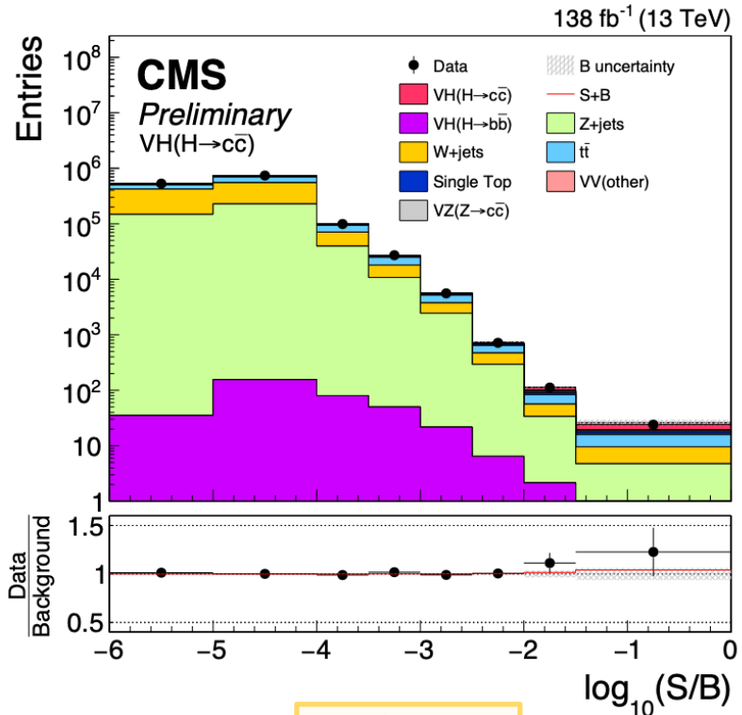

combination

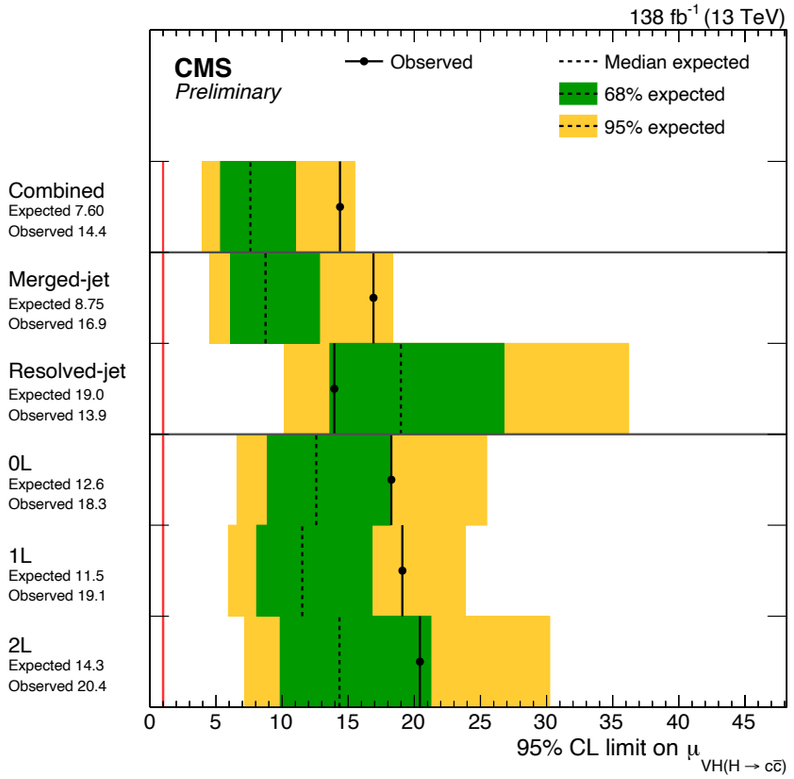

Upper limits on the VH(H → cc) signal strength at 95% CL

- **$\mu_{VH(H \to cc)} < 14\ (7.6)$** observed (expected)
- setting stronger limit w.r.t. ATLAS full Run 2 result $\mu_{VH(H \to cc)} < 26\ (31)$ obs. (exp.) [arXiv:2201.11428]

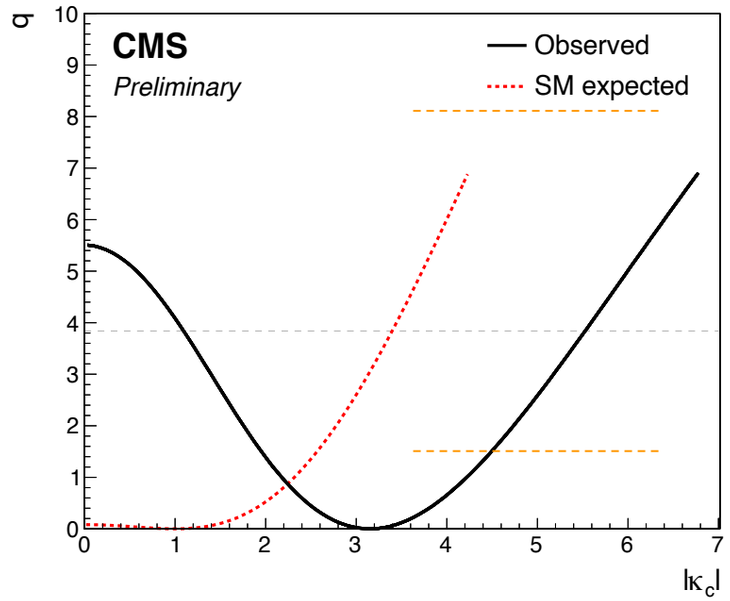

95% CL interval on κ_c:

$1.1 < |\kappa_c| < 5.5\ (|\kappa_c| < 3.4)$ observed (expected)

Projection at HL-LHC

➔ Strategy for **merged-jet topology** extrapolated to HL-LHC (3000 fb^{-1})

- **simultaneous extraction of H→bb and H→cc signal strength**
- based on Run 2 analysis and add new categories enriched for H→bb; lower the pT threshold to 200 GeV → increase the signal acceptance

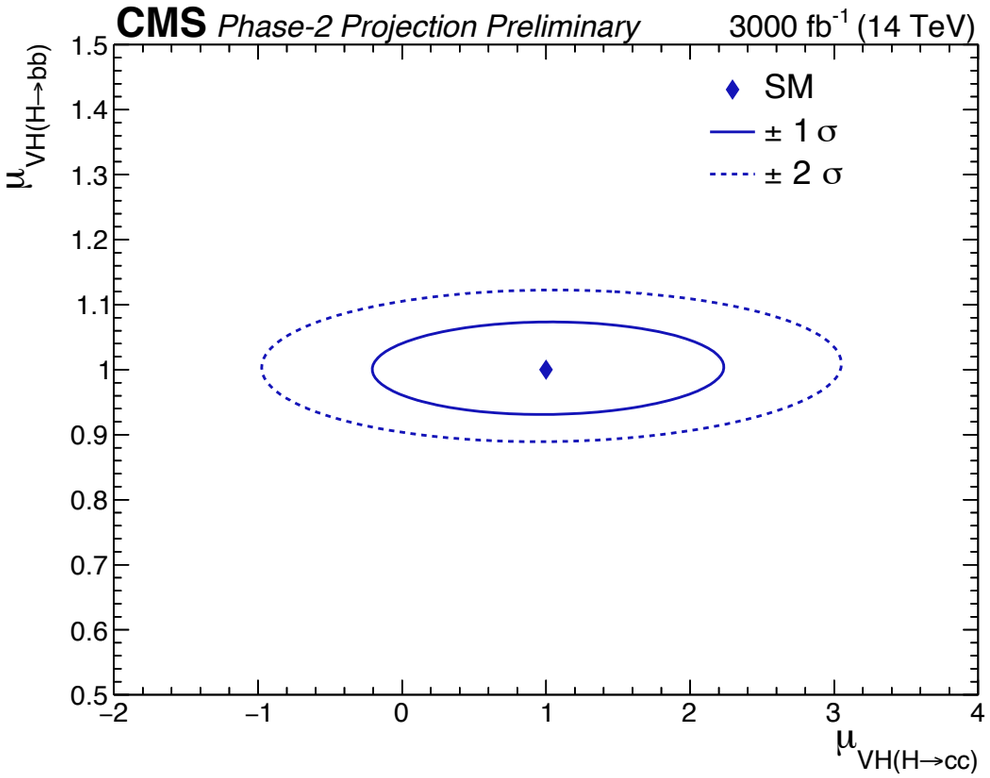

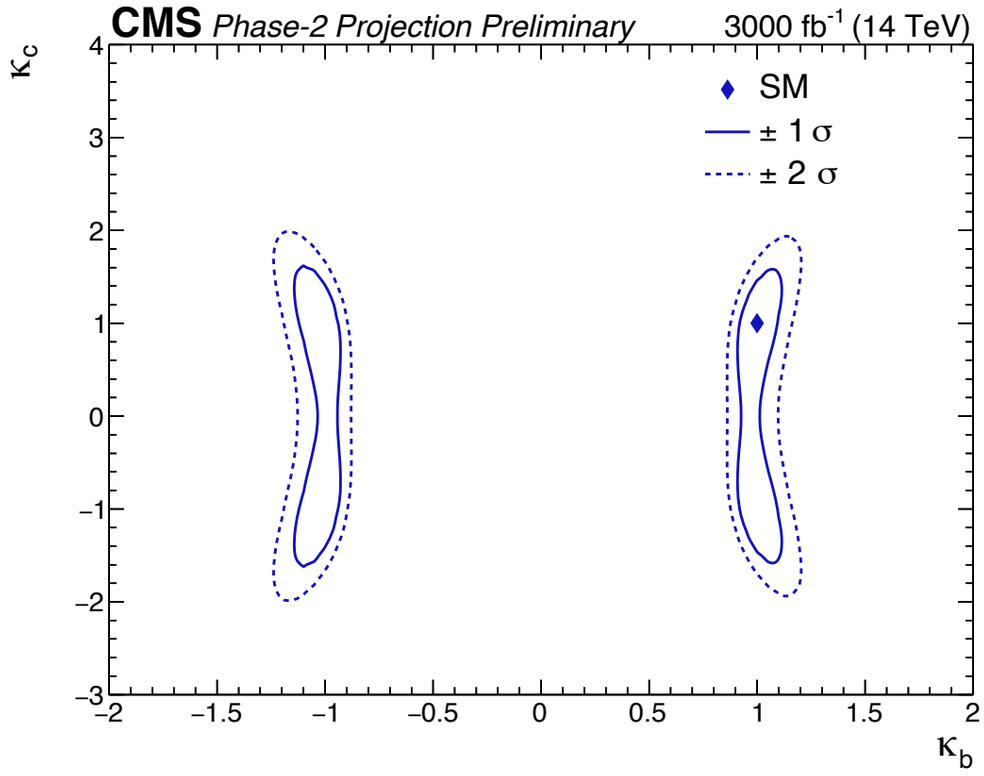

- $\mu_{VH(H \to bb)}$ = 1.00 ± 0.03 (stat.) ± 0.04 (syst.) = 1.00 ± 0.05 (total)
- $\mu_{VH(H \to cc)}$ = 1.0 ± 0.6 (stat.) ± 0.5 (syst.) = 1.0 ± 0.8 (total)

⇨ **Expected sensitivity reach ~*o*(0.1-1) level with the use of novel tagger and strategy**

Summary

➔ The search of H→cc in the VH production mode using full Run 2 data is presented

- ❖ use two complementary approaches: **resolved- & merged-jet topology** to fully explore the VH(H→cc) decay phase-space
  - ▸ results combined to further improve the sensitivity
- ❖ exploit advanced **DNN-based charm & di-charm jet taggers**
  - ▸ **huge performance gains** in charm tagging with the new ML techniques
- ❖ explore DNN-based method for **jet mass/energy regression**

➔ The full analysis procedure validated by measuring VZ(Z→cc)

- ❖ establish the first observation of Z→cc on a hadron collider: significance at 5.7σ
- ❖ set the most stringent limit on VH(H→cc)
  - ▸ upper limit on 95% CL: $\mu_{VH(H \to cc)} < 14$ (7.6) observed (expected)
  - ▸ pave the way to possibly a real observation of H→cc in the future

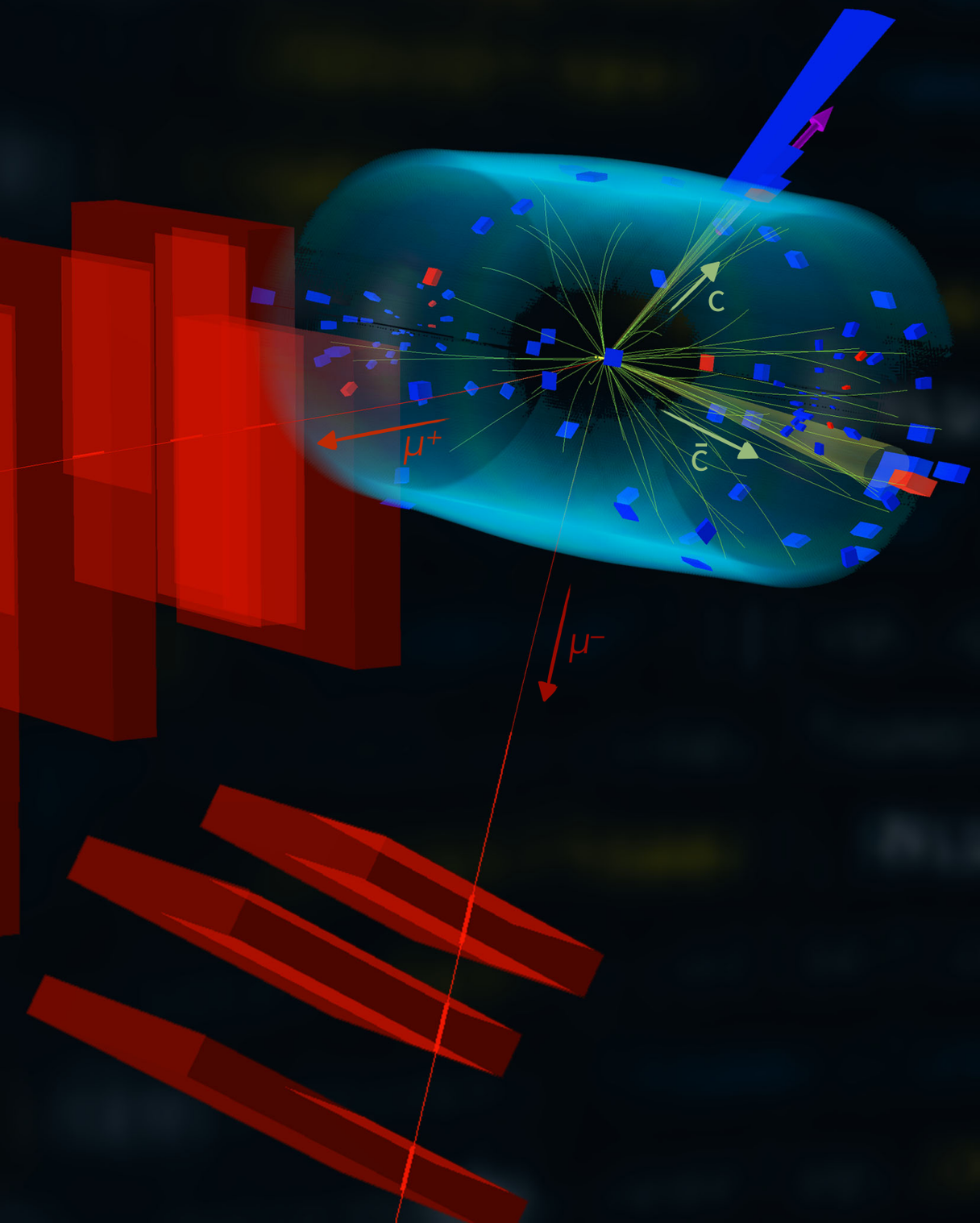

Backup

Higgs-charm coupling at HL-LHC

➔ Expected sensitivity at HL-LHC [CERN-2019-007]

H→cc decay	$\lvert\kappa_c\rvert$ < ~1-2
cH production	$\lvert\kappa_c\rvert$ < ~2-3
H→J/Ψγ	$\lvert\kappa_c\rvert$ < ~80
p_T(H) distribution	$\lvert\kappa_c\rvert$ < ~10
WH charge assymetry	$\lvert\kappa_c\rvert$ < ~4-5

ATLAS HL-LHC projection for H→cc

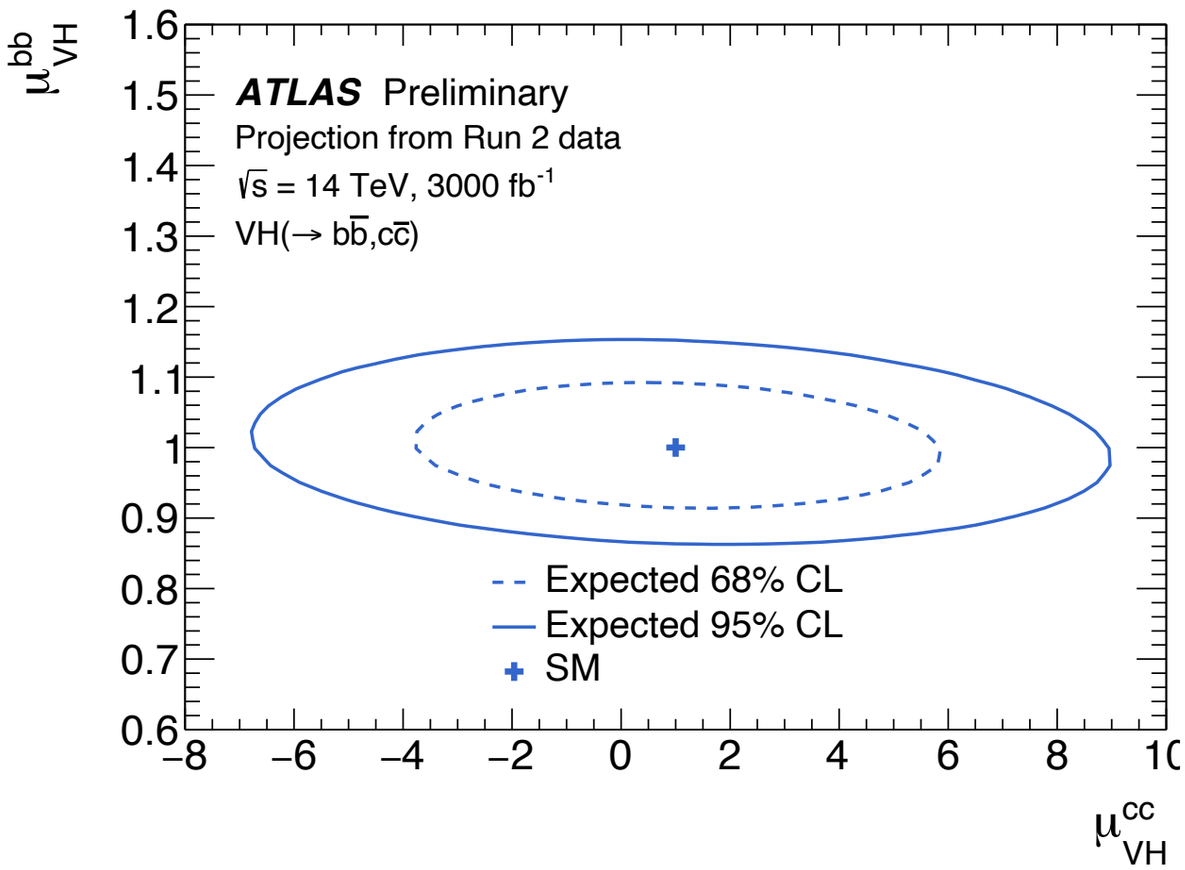

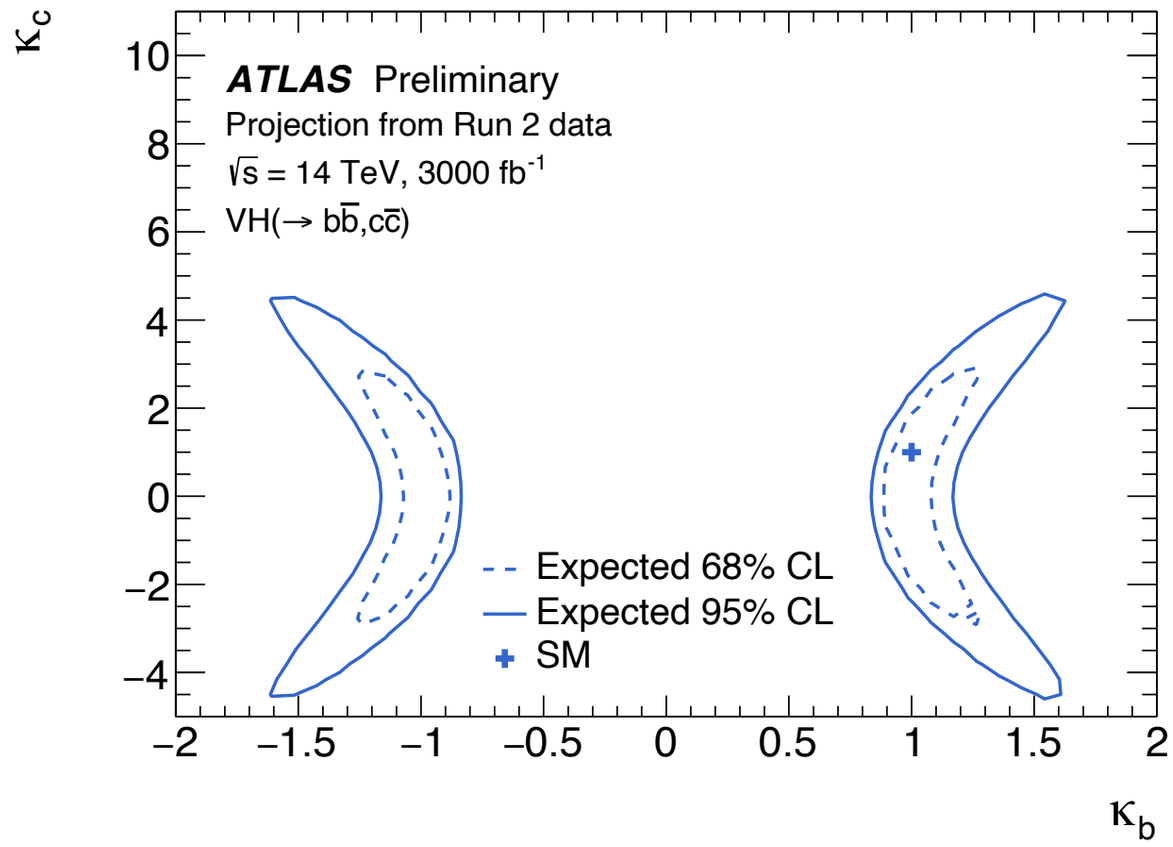

Baseline event selection

Merged-jet topology

Variable	0L	1L	2L
p_{T}^{ℓ}	—	(>25,>30)	>20
Lepton isolation	—	(<0.06, —)	(<0.25, —)
$N_{a\ell}$	=0	=0	—
$M(\ell\ell)$	—	—	75–105
$N^{aj}_{\text{small-}R}$	<2	<2	<3
$p_{\mathrm{T}}^{\mathrm{miss}}$	>200	>60	—
$p_{\mathrm{T}}(\mathrm{V})$	>200	>150	>150
$p_{\mathrm{T}}(\mathrm{H_{cand}})$	>300	>300	>300
$m\,(\mathrm{H_{cand}})$	50–200	50–200	50–200
$\Delta\phi(\mathrm{V},\mathrm{H_{cand}})$	>2.5	>2.5	>2.5
$\Delta\phi(\vec{p}_{\mathrm{T}}^{\mathrm{miss}},\mathrm{j})$	>0.5	—	—
$\Delta\phi(\vec{p}_{\mathrm{T}}^{\mathrm{miss}},\ell)$	—	<1.5	—
Kinematic BDT	>0.55	0.55–0.7, >0.7	>0.55
$c\bar{c}$ discriminant			
High purity	>0.99	>0.99	>0.99
Medium purity	0.96–0.99	0.96–0.99	0.96–0.99
Low purity	0.90–0.96	0.90–0.96	0.90–0.96

Resolved-jet topology

Variable	0L	1L	2L low-p_{T}(V)	2L high-p_{T}(V)
p_{T}^{ℓ}	—	(>25,>30)	>20	>20
Lepton isolation	—	(<0.06, —)	(<0.25, —)	(<0.25, —)
$N_{a\ell}$	=0	=0	—	—
$M(\ell\ell)$	—	—	75–105	75–105
$p_{\mathrm{T}}(\mathrm{j}_1)$	>60	>25	>20	>20
$p_{\mathrm{T}}(\mathrm{j}_2)$	>35	>25	>20	>20
$CvsL(\mathrm{j}_1)$	>0.225	>0.225	>0.225	>0.225
$CvsB(\mathrm{j}_2)$	>0.4	>0.4	>0.4	>0.4
$N^{aj}_{\text{small-}R}$	—	<2	—	—
$p_{\mathrm{T}}^{\mathrm{miss}}$	> 170	—	—	—
$p_{\mathrm{T}}^{\mathrm{miss}}$ significance	—	>4	—	—
$p_{\mathrm{T}}(\mathrm{V})$	>170	>100	60–150	>150
$p_{\mathrm{T}}(\mathrm{H_{cand}})$	>120	>100	—	—
$m\,(\mathrm{H_{cand}})$	<250	<250	<250	<250
$\Delta\phi(\mathrm{V},\mathrm{H_{cand}})$	>2.0	>2.5	>2.5	>2.5
$\Delta\phi(\vec{p}_{\mathrm{T}}^{\mathrm{miss}},\mathrm{j})$	>0.5	—	—	—
$\Delta\phi(\vec{p}_{\mathrm{T}}^{\mathrm{miss}},\ell)$	—	<2.0	—	—

Uncertainties

Merged-jet topology

Uncertainty source	$\Delta\mu / (\Delta\mu)_{\text{tot}}$
Statistical	**88%**
Background normalizations	39%
Experimental	**40%**
Sizes of the simulated samples	24%
Charm identification efficiencies	26%
Jet energy scale and resolution	15%
Simulation modeling	1%
Luminosity	5%
Lepton identification efficiencies	2%
Theory	**25%**
Backgrounds	21%
Signal	14%

Resolved-jet topology

Uncertainty source	$\Delta\mu / (\Delta\mu)_{\text{tot}}$
Statistical	**66%**
Background normalizations	28%
Experimental	**72%**
Sizes of the simulated samples	59%
Charm identification efficiencies	27%
Jet energy scale and resolution	17%
Simulation modeling	20%
Luminosity	13%
Lepton identification efficiencies	10%
Theory	**22%**
Backgrounds	21%
Signal	7%

Datasets and MC samples

- ➔ Datasets and triggers
  - ❖ 138 fb^{-1} for full Run 2 data
  - ❖ **0L**: MET dataset + MET_MHT triggers
  - ❖ **1L**: SingleElectron/SingleMuon dataset + single-e/μ triggers
  - ❖ **2L**: DoubleEG/DoubleMuon dataset + double-e/μ triggers
    - ▸ (merged-jet analysis uses single-e/μ datasets and triggers)
- ➔ Simulated samples
  - ❖ **W/Z+jets**: MadGraph5 NLO samples
  - ❖ **$t\bar{t}$**: POWHEG NLO sample
  - ❖ **single top**: POWHEG/MadGraph5 NLO samples
  - ❖ **VV**: POWHEG/MadGraph5 NLO samples (NNLO QCD & NLO EW correction on $p_T(V_2)$)
  - ❖ **VH signals**: POWHEG NLO samples (NLO EWK $p_T(V)$ correction; NNLO cross section)
- ➔ Corrections
  - ❖ lepton efficiencies, JEC/JER, pileup reweighting, MET filters, c-tagging, etc.

DeepJet details

Resolved

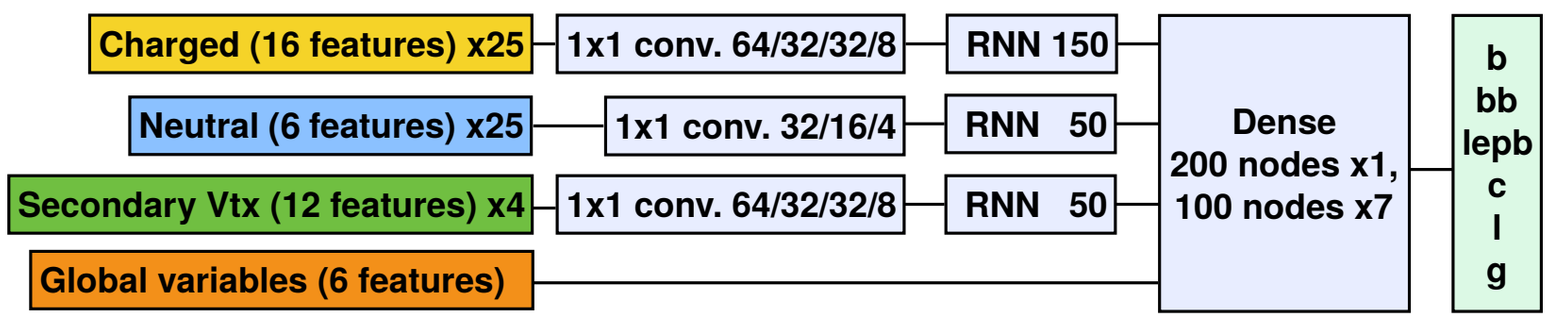

DeepJet architecture [JINST 15 (2020) P12012]

➔ Use low-level features (PF candidates, SV) as well as global features

➔ Model architecture:

- ❖ separate 1D CNNs to process three low-level feature classes
  - ▸ for each class, concatenate multiple CNNs with decreasing dimensions
  - ▸ compress the features to lower dimensional space
- ❖ RNNs (LSTM type) applied after CNNs
  - ▸ better handles the variable length sequence (PF candidates/SV)
- ❖ fully connected layer to connect all channels

➔ Output score:

- ❖ 6 raw scores: bb, b (hadronically decay B-hadron), b_{lep} (leptonically decay B-hadron), c, light (uds), gluon
- ❖ construct CvsB, CvsB used in VHcc analysis

DeepJet discriminant

	BvsC/L	CvsB	CvsL
DeepJet:	$P(b)+P(bb)+P(b_{lep})$	$\frac{P(c)}{P(c)+P(b)+P(bb)+P(b_{lep})}$	$\frac{P(c)}{P(c)+P(uds)+P(g)}$

DeepJet performance

Resolved

2016 2017 2018

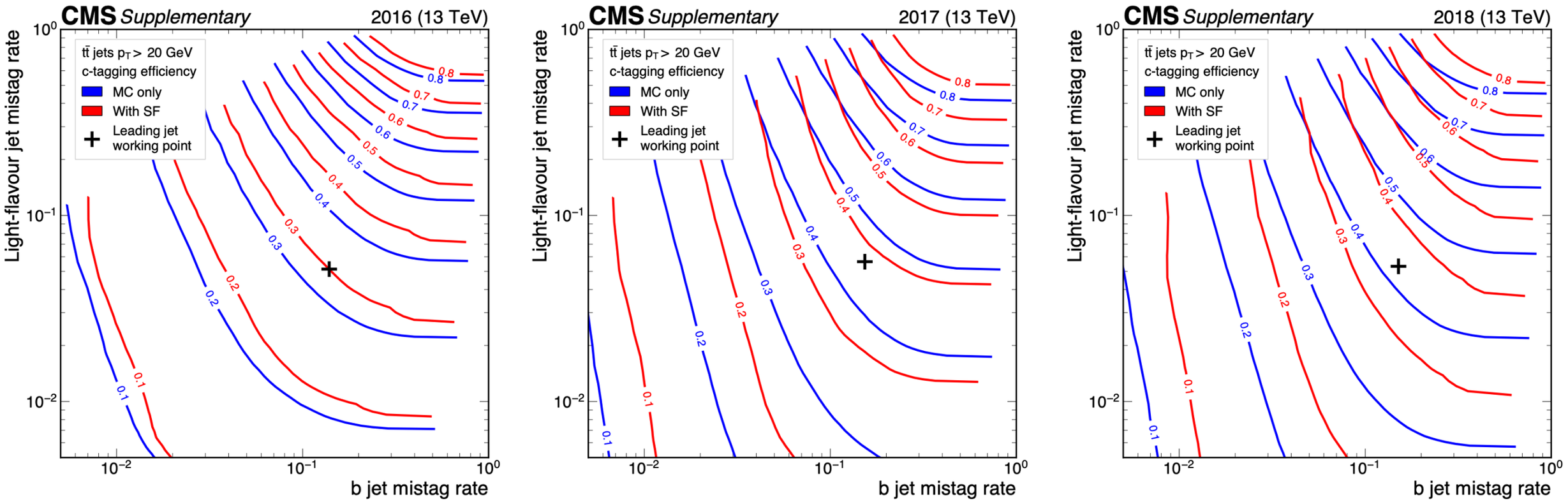

➔ CMS c-tagging WP: ~40% (c), ~16% (b), ~4% (light)

➔ ATLAS c-tagging WP: ~27% (c), 8% (b), 1.6% (light) [arXiv:2201.11428]

Charm tagging calibration

Resolved

- ➔ Per-jet SFs derived as a 3D function of CvsL score, CvsB score, and 3 true flavours
  - ❖ 3 selections pure in b, c, and light jets
  - ❖ iteratively fit in 3 selected phase-space to find simultaneous corrections for all 3 flavours
    - ▸ Z(ℓℓ) + jets (light jet enriched)
    - ▸ W + c (c-jet enriched)
    - ▸ $t\bar{t}$ (b-jet enriched)
- ➔ Propagate to analysis
  - ❖ per-event weight calculated as ***products*** of SF_i(flavour, CvsL, CvsB) for all jet i

DeepJet SFs for year 2017 JINST 17 (2022) P03014

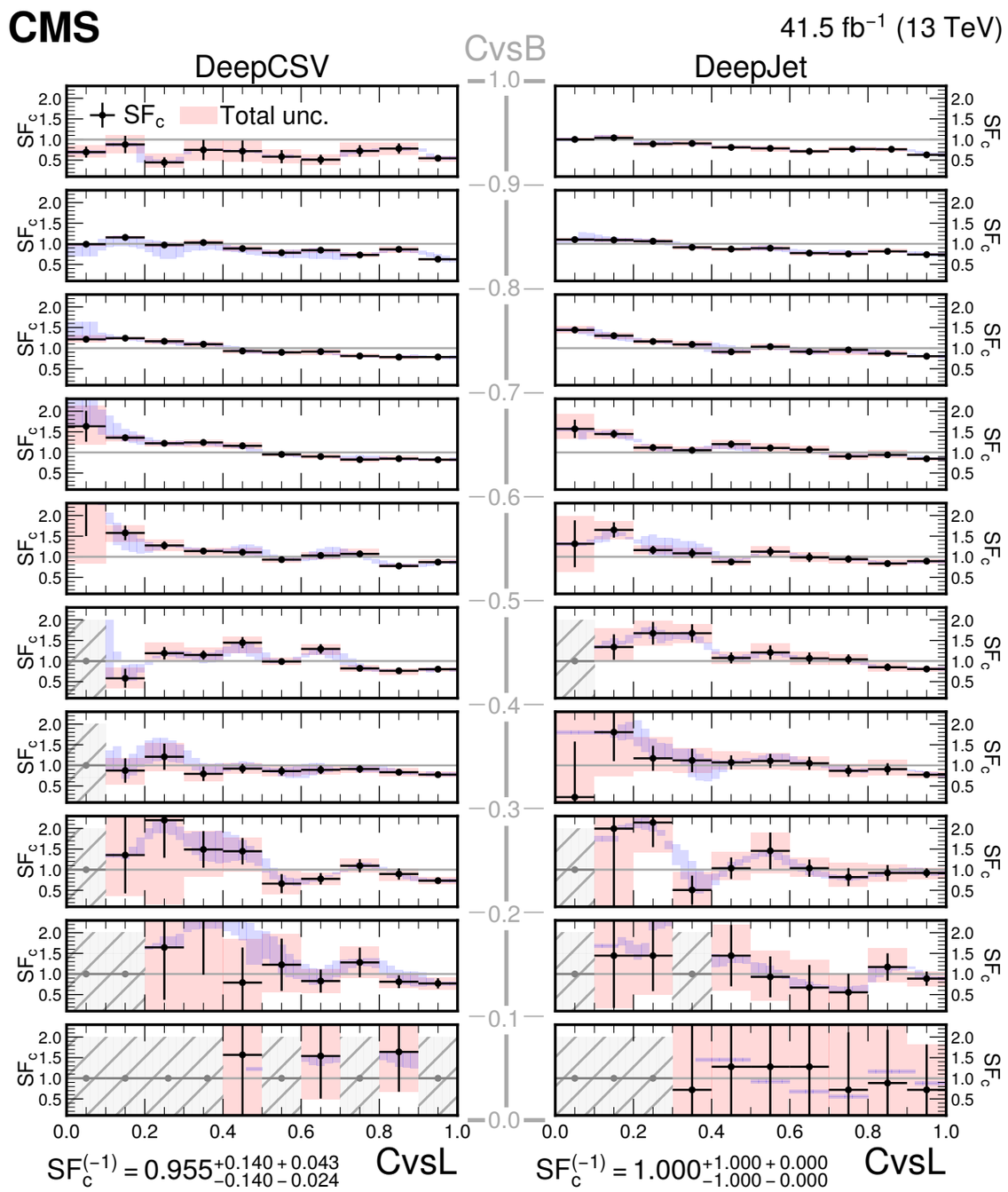

Kinematic fit & signal extraction BDT for resolved-jet

Resolved

➔ Kinematic fit (KinFit) in 2L channel

- ❖ to achieve more precise jet p_T measurement and improve Higgs mass resolution by 30%

KinFit topology

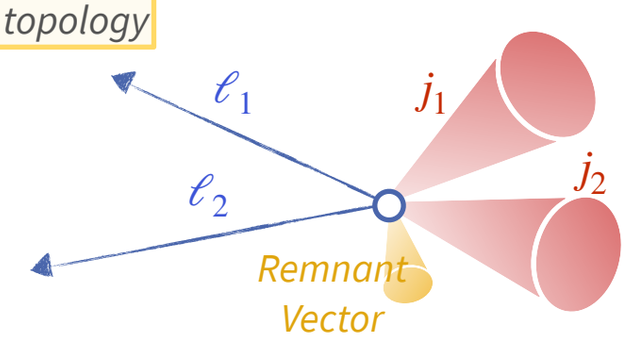

- ❖ apply the fit by:
  - constrain di-lepton system to Z mass
  - balance the $\ell\ell$+cc system in (p_x, p_y) plane
  - allow $p_{T,j1,2}$ to adjust within the uncertainties
  - add recoil jets in the p_T-constraint if they are present

➔ BDTs are trained in 4 categories, 3 years separately to discriminate VHcc signal vs. backgrounds

- ❖ to maximize the sensitivity
- ❖ **BDT used as the fit variable** in SR to extract the VHcc signal

BDT training variables

	Variable	Description	0L	1L	2L
Higgs and vector boson properties	$m(\mathrm{H})$	H mass	✓	✓	✓
	$p_\mathrm{T}(\mathrm{H})$	H transverse momentum	—	✓	✓
	$p_\mathrm{T}(\mathrm{V})$	vector boson transverse momentum	—	✓	✓
	$m_\mathrm{T}(\mathrm{V})$	vector boson transverse mass	—	✓	—
	$p_\mathrm{T}^\mathrm{miss}$	missing transverse momentum	✓	✓	—
	$p_\mathrm{T}(\mathrm{V})/p_\mathrm{T}(\mathrm{H})$	ratio between vector boson and H transverse momenta	✓	✓	✓
c-tagging score	$CvsL_\mathrm{max}$	*CvsL* value of the leading *CvsL* jet	✓	✓	✓
	$CvsB_\mathrm{max}$	*CvsB* value of the leading *CvsL* jet	✓	✓	✓
	$CvsL_\mathrm{min}$	*CvsL* value of the subleading *CvsL* jet	✓	✓	✓
	$CvsB_\mathrm{min}$	*CvsB* value of the subleading *CvsL* jet	✓	✓	✓
event kinematics	p_Tmax	p_T of the leading *CvsL* jet	✓	✓	✓
	p_Tmin	p_T of the subleading *CvsL* jet	✓	✓	✓
	$\Delta\phi(\mathrm{V},\mathrm{H})$	azimuthal angle between vector boson and H	✓	✓	✓
	$\Delta R(\mathrm{j}_1,\mathrm{j}_2)$	ΔR between leading and subleading *CvsL* jets	—	✓	✓
	$\Delta\phi(\mathrm{j}_1,\mathrm{j}_2)$	azimuthal angle between leading and subleading *CvsL* jets	✓	✓	—
	$\Delta\eta(\mathrm{j}_1,\mathrm{j}_2)$	difference in pseudorapidity between leading and subleading *CvsL* jets	✓	✓	✓
	$\Delta\phi(\ell_1,\ell_2)$	azimuthal angle between leading and subleading p_T leptons	—	—	✓
	$\Delta\eta(\ell_1,\ell_2)$	difference in pseudorapidity between leading and subleading p_T leptons	—	—	✓
	$\Delta\phi(\ell_1,\mathrm{j}_1)$	azimuthal angle between leading p_T lepton and leading *CvsL* jet	—	✓	—
	$\Delta\phi(\ell_2,\mathrm{j}_1)$	azimuthal angle between subleading p_T lepton and leading *CvsL* jet	—	—	✓
	$\Delta\phi(\ell_2,\mathrm{j}_2)$	azimuthal angle between subleading p_T lepton and subleading *CvsL* jet	—	—	✓
	$\Delta\phi(\ell_1,p_\mathrm{T}^\mathrm{miss})$	azimuthal angle between leading p_T lepton and missing transverse momentum	—	✓	—
	$\sigma_{cReg}(\mathrm{j}_1)$	leading p_T jet resolution from c-jet energy regression	✓	✓	✓
	$\sigma_{cReg}(\mathrm{j}_2)$	subleading p_T jet resolution from c-jet energy regression	✓	✓	✓
Variables from KinFit (for 2L only)	$\Delta\eta(\mathrm{V},\mathrm{H})\|_\mathrm{kinfit}$	difference in pseudorapidity between vector boson and H, after kinematic-fit	—	—	✓
	$\Delta\phi(\mathrm{V},\mathrm{H})\|_\mathrm{kinfit}$	azimuthal angle between vector boson and H, after kinematic-fit	—	—	✓
	$m(\mathrm{H})\|_\mathrm{kinfit}$	H mass after kinematic-fit	—	—	✓
	$p_\mathrm{T}(\mathrm{H})\|_\mathrm{kinfit}$	H transverse momentum after kinematic-fit	—	—	✓
	$p_\mathrm{Tmax}\|_\mathrm{kinfit}$	p_T of the leading *CvsL* jet after kinematic-fit	—	—	✓
	$p_\mathrm{Tmin}\|_\mathrm{kinfit}$	p_T of the subleading *CvsL* jet after kinematic-fit	—	—	✓
	$p_\mathrm{T}(\mathrm{V})/p_\mathrm{T}(\mathrm{H})\|_\mathrm{kinfit}$	ratio between vector boson and H transverse momenta after kinematic-fit	—	—	✓
	$\sigma(\mathrm{H})\|_\mathrm{kinfit}$	H invariant mass resolution from kinematic fit	—	—	✓

ParticleNet architecture and inputs

Merged

➔ ParticleNet harness the Dynamic Graph CNN (DGCNN) [arXiv:1801.07829]

- ❖ harness EdgeConv operation to pass on learned features for each point which is interpreted as “coordinates” in high-dim latent space
- ❖ increasing layer size for EdgeConv
- ❖ fully connected layer transfer the feature space to N outputs

➔ Input feature

- ❖ up to 100 PF candidates per jet with 20 features + 2 coordinates (η_{rel}, ϕ_{rel})
- ❖ up to 10 SVs per jet with 11 features + 2 coordinates (η_{rel}, ϕ_{rel})

➔ Training performed by the framework `weaver`

➔ More details in [CMS-DP-2020-002]

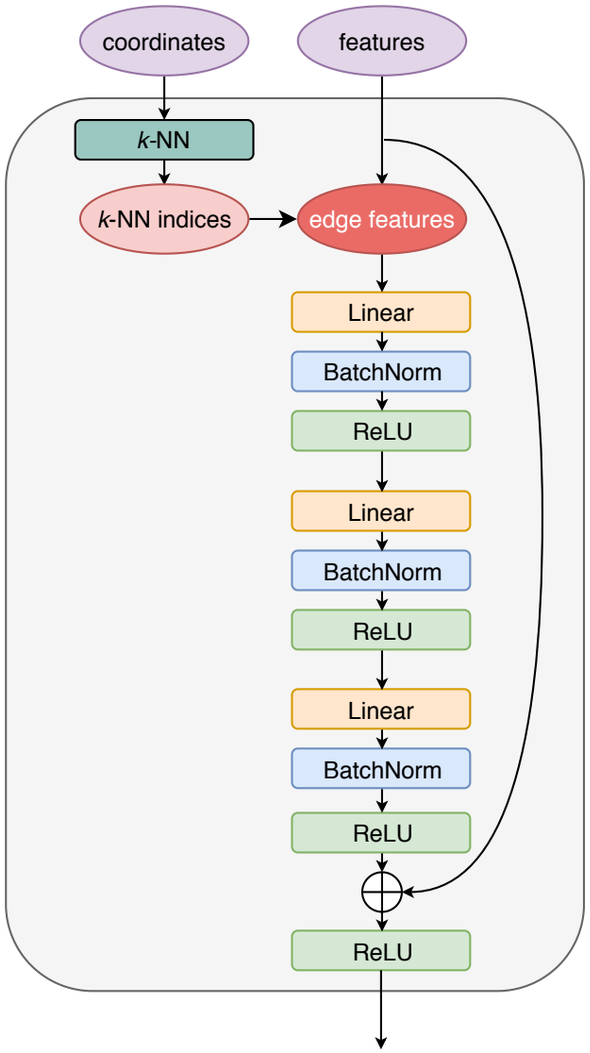

EdgeConv block

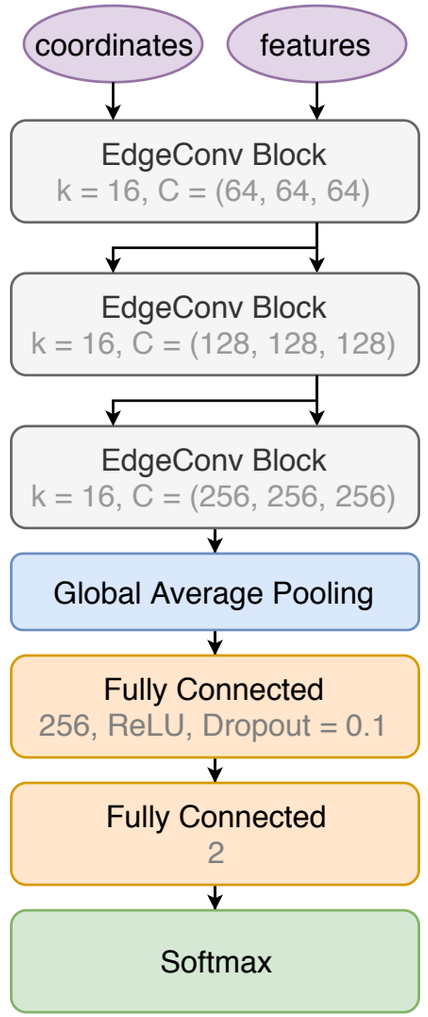

ParticleNet full architecture

Merged

ParticleNet calibration

- ParticleNet tagger calibration for H→cc signal jet
  - use g→cc from QCD multi-jet events as a proxy to H→cc jets
  - ***sfBDT***: select a phase-space from g→cc that resembles H→cc jets
    - provide a handle to adjust the proxy–signal jet similarity
  - simultaneous fit in pass and fail tagger region
    - fit variable: $\log(m_{SV})$
    - 3 rate parameters for c(cc), b(bb), light
    - improved treatment of the systematics
  - details in [CMS-DP-2022-005]

Passing category

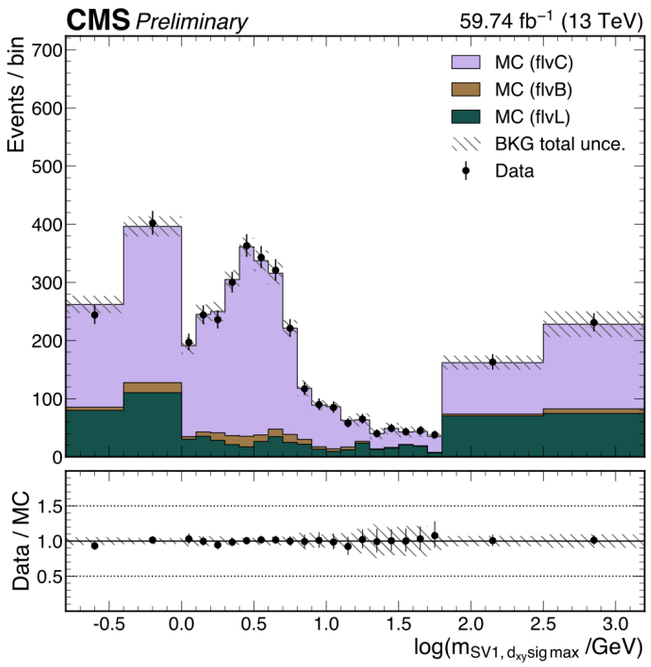

Failing category

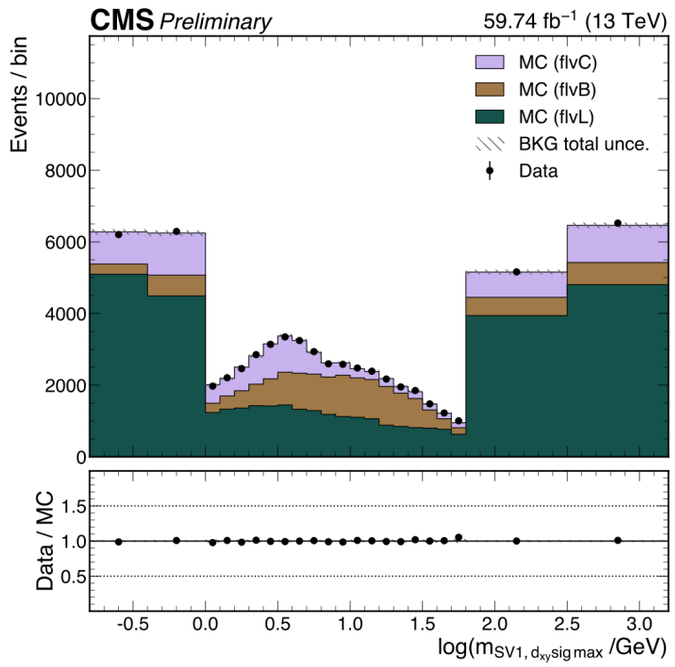

cc-tagging scale factors

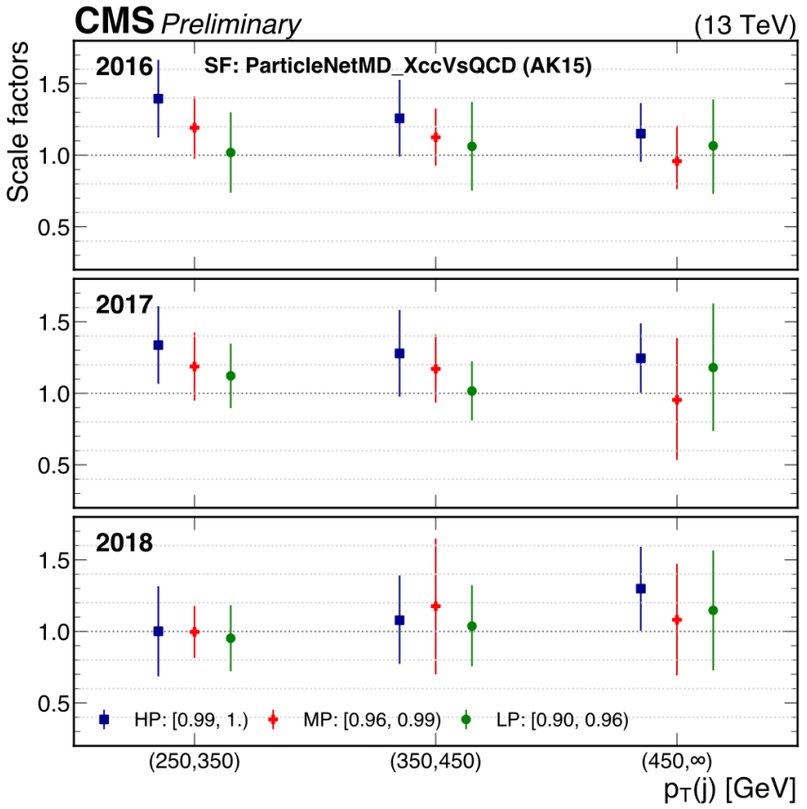

Merged

kinematic BDT for merged-jet topology

- ➔ Kinematic BDT developed to better separate VH signals from major backgrounds (V+jets, $t\bar{t}$)
  - ❖ using only event kinematics, not intrinsic property (e.g. mass/flavour) of the AK15 jets
    - ▸ BDT largely uncorrelated with m_{reg} and ParticleNet cc-tagger
  - ❖ low-BDT CR defined based on kinematic BDT

inclusive BDT distribution for 3 channels

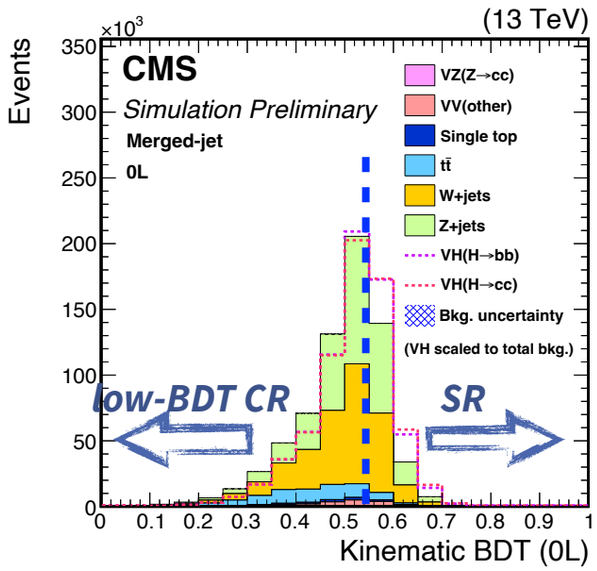

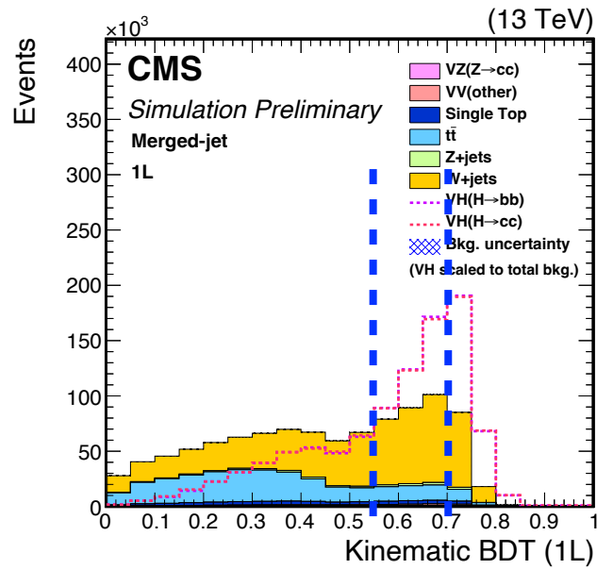

input variables to kinematic BDT

Variable	Description	0-lepton	1-lepton	2-lepton
$p_T(V)$	vector boson transverse momentum	✓	✓	✓
$\Delta R(\ell,\ell)$	angular separation between the two leptons			✓
p_T (H_{cand})	H_{cand} transverse momentum	✓	✓	✓
$\lvert\eta(H_{cand})\rvert$	absolute value of the H_{cand} pseudorapidity	✓		
$\Delta\phi(V, H_{cand})$	azimuthal angle between vector boson and H_{cand}	✓	✓	✓
p_T^{miss}	missing transverse momentum		✓	
$\Delta\eta(H_{cand},\ell)$	difference in pseudorapidity between H_{cand} and the lepton		✓	
$\Delta\eta(H_{cand},V)$	difference in pseudorapidity between H_{cand} and vector boson			✓
$\Delta\eta(H_{cand},j)$	min. difference in pseudorapidity between H_{cand} and small-R jets	✓	✓	✓
$\Delta\eta(\ell,j)$	min. difference in pseudorapidity between the lepton and small-R jets		✓	
$\Delta\eta(V,j)$	min. difference in pseudorapidity between vector boson and small-R jets			✓
$\Delta\phi(\vec{p}_T^{miss},j)$	azimuthal angle between $\vec{p}_T^{miss}$ and closest small-R jet	✓		
$\Delta\phi(\vec{p}_T^{miss},\ell)$	azimuthal angle between $\vec{p}_T^{miss}$ and lepton		✓	
m_T	transverse mass of lepton $\vec{p}_T$ + $\vec{p}_T^{miss}$		✓	
N_j	number of small-R jets	✓	✓	✓